PACIFIC EARTHQUAKE ENGINEERING RESEARCH CENTER

Semi-Automated Procedure for Windowing Time Series and Computing Fourier Amplitude Spectra for the NGA-West2 Database

Tadahiro Kishida

Olga-Joan Ktenidou

Pacific Earthquake Engineering Research Center

Robert B. Darragh

Walter J. Silva

Pacific Engineering & Analysis
El Cerrito, California

PEER Report No. 2016/02
Pacific Earthquake Engineering Research Center
Headquarters at the University of California, Berkeley

May 2016

PEER 2016/02
May 2016

Semi-Automated Procedure for Windowing Time Series and Computing Fourier Amplitude Spectra for the NGA-West2 Database

Tadahiro Kishida

Olga-Joan Ktenidou

Pacific Earthquake Engineering Research Center
University of California, Berkeley

Robert B. Darragh

Walter J. Silva

Pacific Engineering and Analysis

PEER Report 2016/02
Pacific Earthquake Engineering Research Center
Headquarters at the University of California, Berkeley

May 2016

ABSTRACT

This document introduces and describes the data processing methods developed for computing Fourier amplitude spectra (FAS) in the NGA-West2 project. The products of this study can be used to estimate high-frequency attenuation, kappa (κ), to estimate site amplification through empirical spectral ratios, as well as to aid in the development of ground-motion models (GMMs) based on FAS. To accommodate different potential user objectives, we selected five time windows in the acceleration time series (noise, *P*-wave, *S*-wave, coda, and the entire record) for which we compute the FAS. The processing starts with the time-aligned, instrument-corrected, tapered, and filtered acceleration time series. The proposed window selection method is developed through trial and error, and tested against a range of ground motions with different magnitudes and hypocentral distances from different regions. This document summarizes the steps for window selection and FAS computation, and describes the output data format. This report will be accompanied by the final products of the PEER NGA-West2 Project, namely, the published report describing the database [Ancheta et al. 2013] and the flatfile, which can be downloaded in excel format at: *http://peer.berkeley.edu/ngawest2/databases/.*

ACKNOWLEDGMENTS

The authors are grateful to Norm Abrahamson and Dave Boore for providing comments and sharing their experiences. This project would not have succeeded without the contribution of Sahar Derakhshan and Sifat Muin, who performed the bulk of the data processing. We acknowledge Yousef Bozorgnia for his leadership and guidance, and Claire Johnson for editing the report. This project was supported primarily by the Pacific Earthquake Engineering Research Center (PEER). Olga-Joan Ktenidou was also partially funded by PG&E, the French Sigma Project, and the GFZ German Research Centre for Geosciences. Any opinions, findings, and conclusions or recommendations expressed in this material are those of the authors and do not necessarily reflect the above organizations.

CONTENTS

LIST OF TABLES

LIST OF FIGURES

1 Methodology for Data Processing

1.1 INTRODUCTION

The Fourier Amplitude Spectrum (FAS) is used in a number of applications, including spectral analysis and inversions, the study of site effects and amplification, the measurement of high-frequency attenuation (kappa, or κ), and the development of predictive ground motion models (GMMs).

In the past, GMMs were most often developed directly from 5% damped pseudo-acceleration response spectra (PSa). Recently, more focus has been placed on GMMs that fit Fourier rather than response spectra. For instance, within the Next Generation Attenuation (NGA) project sponsored by the Pacific Earthquake Engineering Research Center (PEER), FAS models were developed to provide GMMs for PSa, (e.g., PEER. [2015]), based on the inverse random vibration theory. Often, GMMs developed for a certain host region need to be adjusted so that they can be applied to a target region. In such cases, one of the typical adjustments needed is to the κ parameter [Anderson and Hough 1984]. Typically, κ is measured on FAS using various approaches (as summarized in Ktenidou et al. [2014]). Ktenidou et al. [2016] recently studied κ for rock sites in the NGA-East database [Goulet et al. 2014].

Based on these experiences, PEER recognizes the importance of computing FAS for the NGA-West2 database, which has been used by researchers and practitioners worldwide following its publication [Ancheta et al. 2013]. The computation of FAS for the NGA-West2 database is unique because it includes more than 60,000 records that have been already processed with instrument corrections, filtering, and baseline corrections. Furthermore, different time windows may be of interest for different studies, so another challenge is that the computation of FAS should be performed for different time windows (e.g., *P*-wave, *S*-wave, and coda, etc.). This report describes the semi-automated procedure developed to compute FAS for large databases. It is calibrated so that the majority of visual checks and basic processing can be implemented by less experienced analysts. For example, this procedure only requires selecting the *P*- and *S*-wave onset; the flagging of events requires further inspection by an experienced analyst. This windowing procedure is explained in the following sections, followed by a description of the FAS computation.

1.2 TIME WINDOWS REQUIRED FOR DATA PROCESSING

Five different time windows were selected from the acceleration time series, as shown schematically in Figure 1.1. The first time window includes the entire record (blue box in the figure), which contains the pre-event noise recorded before the *P*-wave onset, along with the *P*-, *S*-, and coda waves. The second window contains only the pre-event noise (pink box), the third the *P*-waves (yellow box), the fourth the *S*-waves (green box), and the fifth contains the coda waves (gray box). All windows are selected during the processing stage to provide the time windows used in the FAS calculation. Not all time windows are available for all records—for example, due to late trigger and limitation of record length—but as late *S*-triggers have been rejected in the NGA-West2 dataset, the first (entire) and fourth (*S*-wave) windows are always available for any record herein. All windows are explained in more detail in the following sections, following an overview of the semi-automated processing procedure conducted by the analyst.

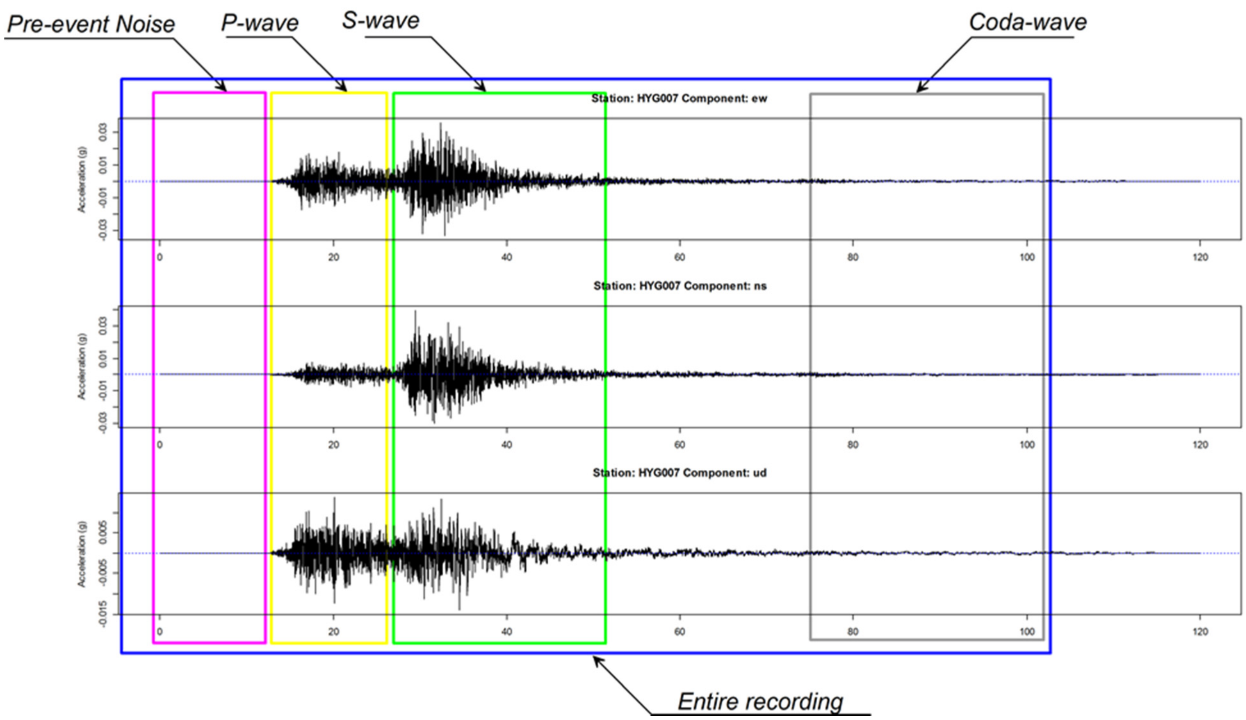

Figure 1.1 **The five time windows extracted from a sample time series (Tottori earthquake, HYG007). The vertical (UD) component is the bottom trace.**

1.3 OVERVIEW OF THE DATA PROCESSING METHOD

A brief overview of the data processing method is given in this section, while the details of the steps are explained in the following sections. The data processing method consists of the following four steps.

- Step 1: First, the analyst visually inspects the tapered and filtered acceleration time histories. If there is a problem (e.g., late trigger), then the wave forms are not accepted. Similar quality checks have been done in the NGA-West1 [Chiou et al. 2008] and NGA-West2 projects [Ancheta et al. 2013]; therefore, we expect virtually all records to be accepted in this process. Since standard PEER processing [Chiou et al. 2008] tapers the acceleration time histories at the beginning of the record, late-triggered records are often difficult to determine. Therefore, recordings previously flagged as late *P*- or *S*-wave triggered recordings should be re-examined by an experienced analyst. If the analyst believes the *S*-wave onset to have taken place before the actual triggering of the instrument, then the recording is flagged for further review; for many applications, the entire *S*-wave window is required (e.g., for the estimation of κ). This step also updates column JL "flag for late *S* trigger" in the flatfile [Ancheta et al. 2013].

- Step 2: Next, the analyst must select the *P*-wave onset. The analyst inspects the entire time series zooms in on the arrival of the *P*-wave with an enlarged window to facilitate the selection of the first arrival. The analyst picks the *P*-arrival time with a fiducial mark. The processing code will then automatically determine the noise window length. If the noise window length is too short compared to the pre-tapered record length, the processing code flags the record to indicate a possible inadequacy. The definition of the noise window flag is described in the following section. This step may update column JM "flag for late *P* trigger" in the flatfile.

- Step 3: The next screen shows the predicted *S*-wave first arrival as computed by the processing code based on the selected *P*-wave arrival and the hypocentral distance from the flatfile. If, based on that, the analyst believes that an error was made in their initial *P*-wave arrival selection or in late *P*-trigger cases, they have the opportunity to go back to the previous step and re-select the first *P* arrival time. If the estimated and selected *S*-wave first arrivals times are significantly different, then the code automatically flags the record as a possible late *P* trigger. This step again may update flatfile column JM.

- Step 4: Based on the chosen *S*-wave onset, the code computes the expected end of the *S*-wave window, as well as the beginning and the end of the coda window, provided the time series is of sufficient duration. The code will automatically flag the record if the coda time window duration is too small or does not exist. The definition of the coda flag is described in the following section. Even though the analyst cannot modify these windows, they may flag the record if they observe a problem, such as the existence of an aftershock in the *S*-wave or coda windows. An experienced analyst will then reprocess the record and may modify the choice of time windows.

1.4 ENTIRE RECORD TIME WINDOW

The time window for the entire record includes pre-event noise (if available), *P*-wave (if available), *S*-wave, and coda waves (if available), as shown in Figure 1.1. Before developing these time windows, every time series must be reviewed and deemed appropriate or rejected for FAS calculation. For example, if the recording is a late *S*-trigger as determined by the trigger flag in the flatfile or by this project, we will not process the recording. Figure 1.2 shows an example of late *S*-triggered records in NGA-West2 database; Figure 1.2(a) shows the unprocessed (un-tapered) recording, and Figure 1.2(b) shows the processed one with cosine tapering applied at the start of the recording. By comparing these figures, it is difficult to determine whether the recording is late *S*-triggered or not by using only the processed recording. Therefore, all rejected recordings in this process are further reviewed by experienced analysts.

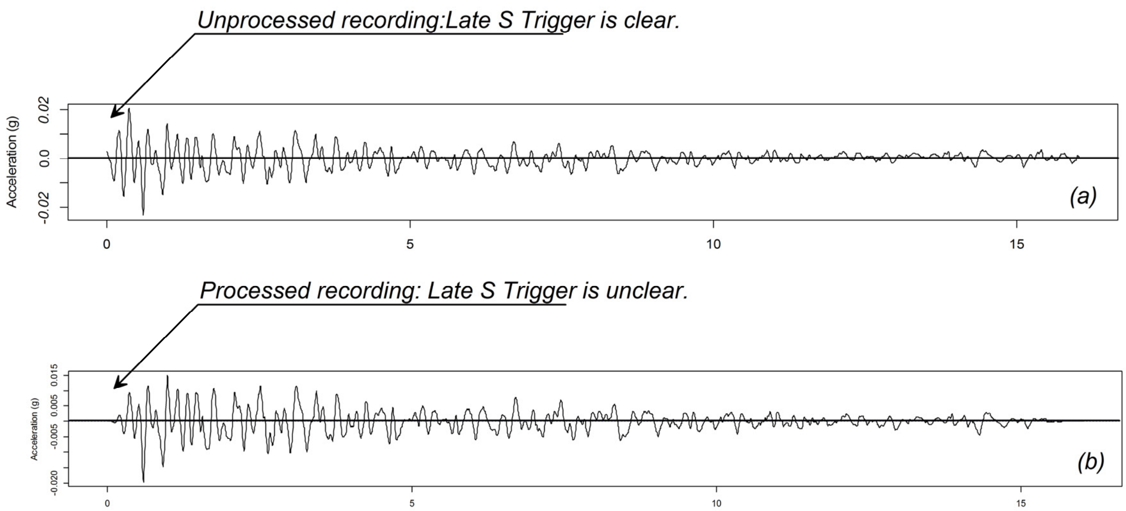

Figure 1.2 Example of a late *S* trigger: to be rejected by the user: (a) unprocessed; and (b) processed recording of Lytle Creek earthquake, Station 24278, 021 component.

1.5 PRE-EVENT NOISE TIME WINDOW

The time window for the pre-event noise is useful in order to compute the signal-to-noise ratio (SNR) of the *S*-wave or other windows, where SNR can be used to assess if the amplitude of the signal is strong enough at a given frequency to use in various applications. However, the existence of a noise window is not an absolute necessity for this purpose: the experienced analyst can also evaluate the quality of the signal by computing SNR with respect to the *P*-wave or coda window (if those are available), or by the shape of the FAS (as low- and high-frequency noise may be identified by increasing amplitude trends in the FAS away from the peak of the spectrum). Therefore, late-*P*-triggered records are not rejected in this study, but the record is flagged if a noise window is unavailable or inadequate (less than about 10 sec).

The start time (t_n) and end time (t_n^f) of the pre-event noise are automatically selected based on the visual pick of the *P*-wave arrival time (t_P) as follows:

$$t_n^f = t_P - 1.0\,\text{sec} \tag{1.1}$$

$$t_n = \max(0, t_n^f - D_S) \tag{1.2}$$

where D_S is the *S*-wave duration defined in the following section. Equation (1.1) shows that the noise window ends 1.0 sec before the *P*-wave arrival, which ensures that initial (e.g., emergent) *P*-wave arrivals are generally excluded from the noise window. The maximum duration of the pre-event noise window is the same as the *S*-wave window duration in Equation (1.2) because the main objective of this window is to compute SNR of the *S*-wave FAS. So the noise window is defined here (contrary to some studies) by first choosing its end, and then its beginning. The typical duration of pre-event noise is 10 sec for most of the processed recordings in the NGA-West2 database (with **M** < 5); hence t_n equals 0 for many of these records.

In selecting the *P*-wave arrival visually, the analyst inspects all three acceleration components. A zoom window option can magnify the 20 sec around the selected *P*-wave arrival time to facilitate precise selection. Figure 1.3 shows the visual inspection of the *P*-wave arrival for the ground motion shown in Figure 1.1. Figures 1.3(a) and 1.3(b) show the entire and the magnified time series, respectively. If the analyst believes the *P*-wave arrival has taken place before the start time of the record, then the *P*-wave arrival selected should be outside of the trace and to the left to indicate a negative time value. In that case, the code will automatically flag the record. The code also automatically flags the record if $t_p \leq 10$ sec, to indicates a possibly inadequate (short) noise window length. This is done to notify the database user that FAS of the noise window could include insufficient spectral resolution because of the tapers applied at the beginning of the record. In general, the beginning taper length in the NGA-West2 project is 1% of the entire record length, although shorter tapers were used especially for vertical recordings from analog instruments. Figure 1.4 shows an example recording with a pre-event noise, which is flagged as 1 based on the following flag definition scheme shown in Equation (1.3):

$$\text{flag} = \begin{cases} -999, & t_p \leq 0\,\text{sec} \\ 1, & 0 < t_p \leq 10\,\text{sec} \\ 0, & t_p > 10\,\text{sec} \end{cases} \tag{1.3}$$

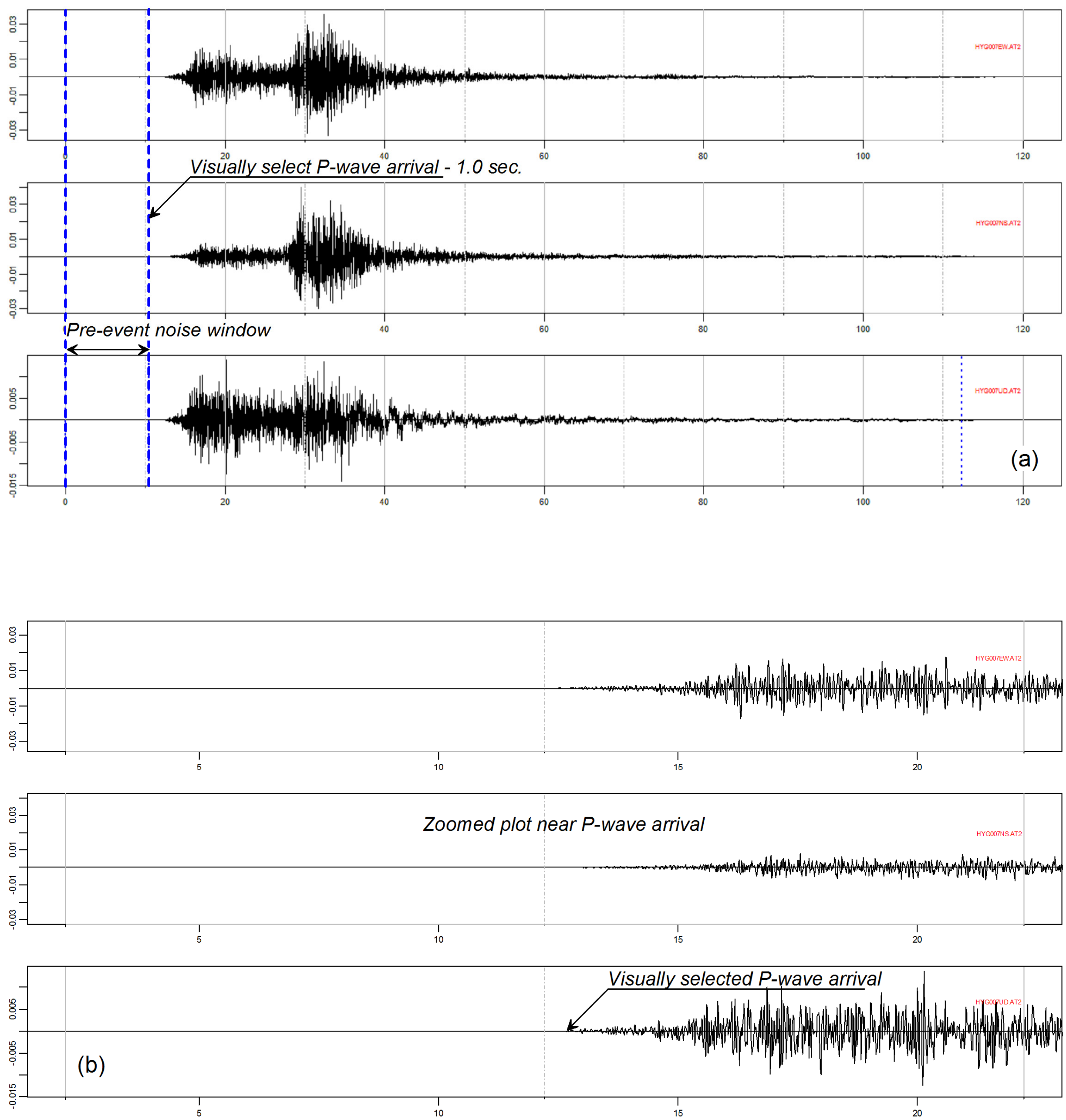

Figure 1.3 Example of visual inspection of *P*-wave arrival time by (a) the entire, and (b) the magnified records. The vertical component is the bottom trace.

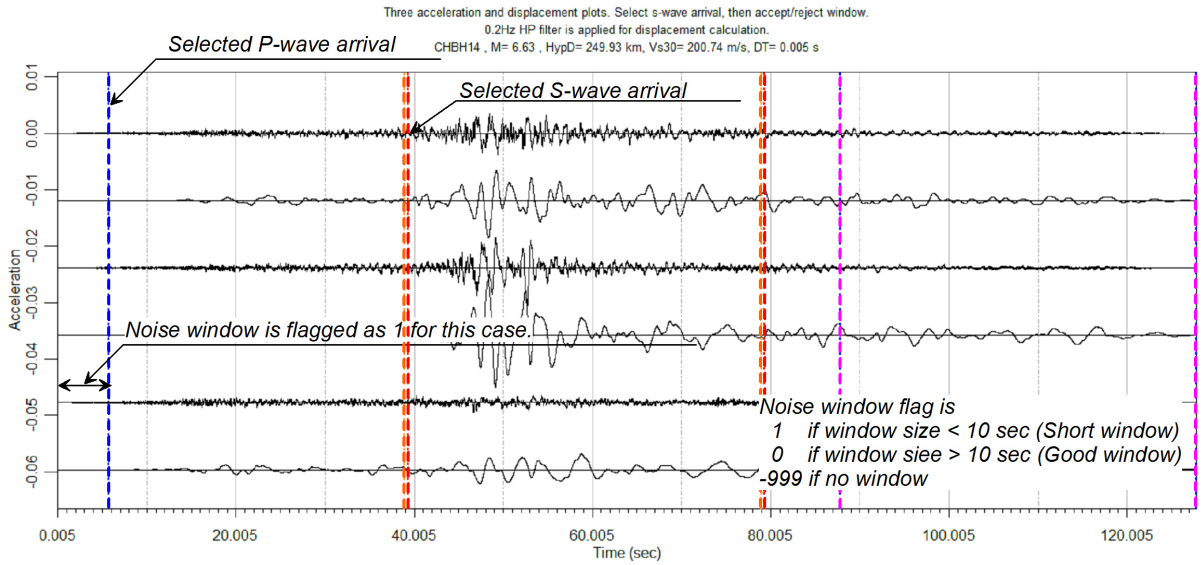

Figure 1.4 **Example of a short noise window with its flag (Niigata earthquake, CHBH14).**

1.6 *P*-WAVE TIME WINDOW

The start time of the *P*-wave window is taken as the end of the noise window defined as t_n^f in Equation (1.1). The end time of the *P*-wave window (t_n^f) is obtained by visual inspection based on the *S*-wave arrival time (t_S) as follows:

$$t_n^f = t_S - 0.5\,\text{sec} \tag{1.4}$$

where 0.5 sec is for the noise taper applied at the start of the *S*-wave window for the FAS calculation. The *S*-wave arrival time is selected visually by the analyst by observing the increase in amplitude and increase in low-frequency content on both the acceleration and displacement time series. As a selection guide, the theoretical *S*-wave arrival time (t_S') is also plotted with the traces. This is automatically computed based on the selected *P*-wave arrival time and the hypocentral distance as follows:

$$t_S' = t_P + \Delta t_{S-P} \approx t_P + R_h/8 \tag{1.5}$$

where R_h is hypocentral distance (in km), and can be obtained from the flatfile [Ancheta et al. 2013]. *P*- and *S*-wave crustal velocities are taken as 6.0 and 3.5 km/sec, respectively, when deriving Equation (1.5). If the selected *P*-wave arrival time is correct, then the *S*-wave arrival time should not differ greatly from the plotted theoretical arrival time, provided the assumed crustal velocities are representative. If it does differ significantly, this may mean that the selected *P*-wave arrival time in the previous step was in error. If the analyst believes they can improve their selection, they have the option to go back a screen and re-select the *P*-wave arrival or onset time. This leads to an updated theoretical *S*-wave arrival time and a new check by the analyst. If the theoretical *S*-wave onset is again not close to the selected *S*-wave arrival time by the analyst, and if the theoretical *S*-wave arrival occurs later than the selected *S* arrival, then the problem is probably due to a late *P*-wave trigger. In this case, the code automatically flags the record as a possible late *P* trigger for an experienced analyst to reprocess. In order to automate this flag, an acceptable difference in the theoretical and selected *S*-wave arrival times had to be determined, which in turn cannot be constant but must depend on distance. For nearby events, the acceptable error must be small (no more than a few seconds); however, for distances of several hundreds of kilometers, the acceptable error may be large, e.g., of the order of several seconds. Hence, after several tests, the limit for an acceptable difference was set at 30% of the Δt_{S-P} in Equation (1.5).

This step also may update column JM of the flatfile (which is the 'flag for late *P* trigger'), along with the pre-event noise flag shown in Figure 1.4. Figure 1.5 shows the comparison of t'_S and t_S for two example recordings. Figure 1.5(a) shows a case where t'_S matches t_S reasonably well, whereas Figure 1.5(b) shows a case where these are significantly different. These cases are flagged as 0 and 1, respectively, based on the following classification scheme:

$$\text{flag} = \begin{cases} 1, & t'_S - t_S \geq 0.3 \cdot R_h / 8 \\ 0, & t'_S - t_S < 0.3 \cdot R_h / 8 \end{cases} \tag{1.6}$$

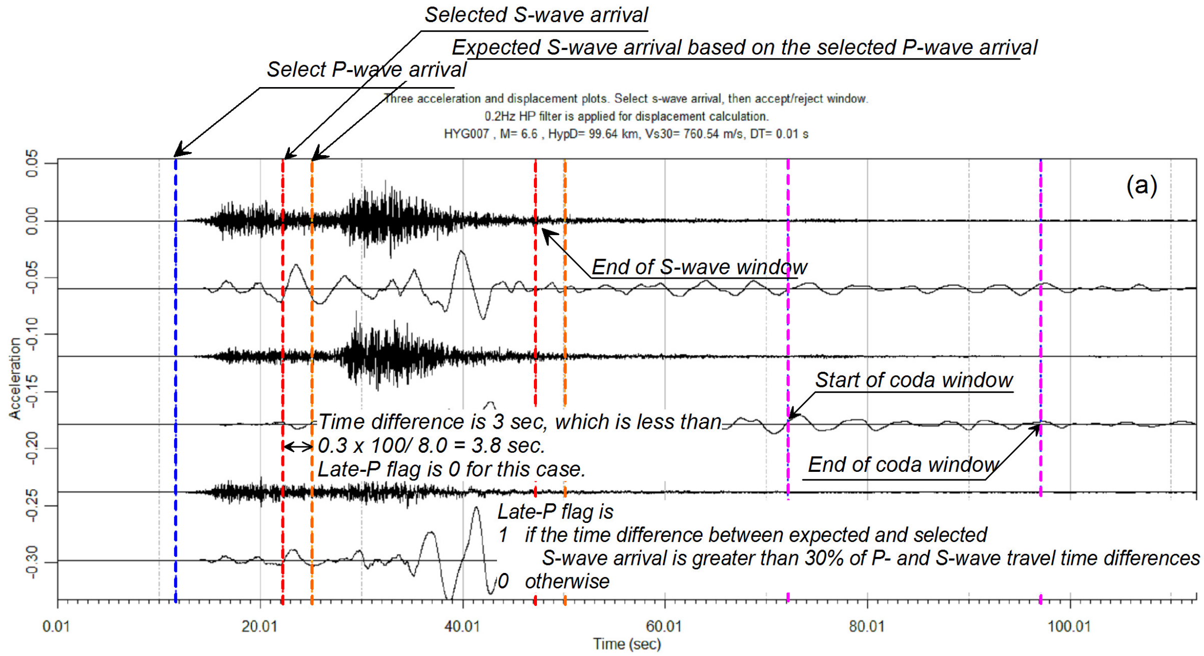

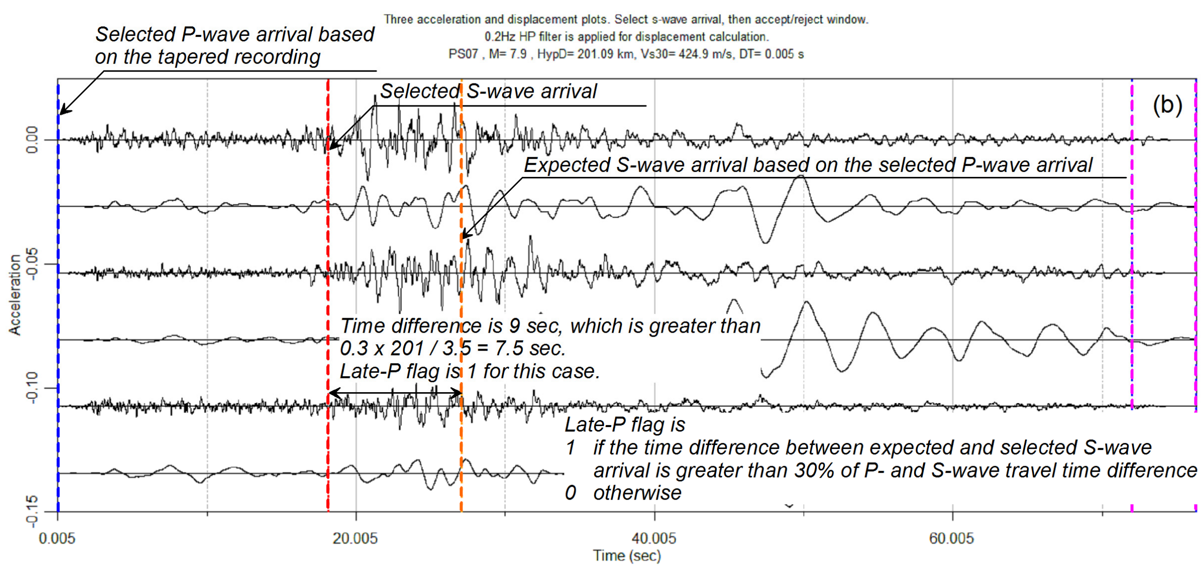

Figure 1.5 **Comparison of the selected *S*-wave arrival (red) with the theoretical *S* arrival (yellow) computed from the selected *P* arrival (blue): (a) the selected *S* arrival matches the theoretical *S* arrival reasonably well; and (b) the selected *S* arrival occurs significantly earlier than the theoretical, indicating a late *P*-triggered record.**

1.7 *S*-WAVE TIME WINDOW

The start time of the *S*-wave window (t_S) is taken as the end of the *P*-wave window (t_P^f), defined in Equation (1.4). The end time of the *S*-wave window is defined as:

$$t_S^f = t_S + D_S \tag{1.7}$$

where D_S is the estimated duration of the *S*-waves (from an extended rupture or other paths) at the recording station. In this project the automatic selection of the *S*-wave window for FAS computation is an important objective. Therefore, it will satisfy this objective if D_S is estimated as reasonably conservative to include all the *S*-wave arrivals. In general, D_S can be written as the sum of two factors:

$$D_S = T_{d-rup} + T_{d-prop} \tag{1.8}$$

where T_{d-rup} is the source rupture duration and $T_{d\text{-}prop}$ the path duration for the propagation of the *S*-wave from the source to the station. T_{d-prop} allows the total observed duration to increase due to wave scattering and multiple paths. T_{d-rup} depends on parameters such as moment magnitude, fault dimensions, rupture velocity, stress drop, and rupture mechanism. For circular rupture, T_{d-rup} is calculated as $1/f_c$, where f_c is the corner frequency of the event [Brune 1970; 1971]. For unilateral rupture, the duration would be twice that value. T_{d-prop} depends on the hypocentral distance and on the structure of the crust, e.g., mainly lateral variations in V_S.

We compared Equation (1.8) against various sets of recordings in a two-step procedure to calibrate the two components. A subset of carefully hand-picked D_S values was created from several events in Greece and the NGA-West2 database—with a range of magnitudes and distances. Acceleration and displacement time series were inspected visually to estimate D_S, where displacement time series were mainly reviewed to judge the *S*-wave duration. More weight was assigned to results obtained from stations with V_{S30} greater than 300 m/sec, as some soft sites may cause an overestimation in the visual *S*-wave duration (possibly due to the generation of strong surface waves in basins).

In Step 1, we plot D_S against distance, in different magnitude bins, for the Greek and NGA-West2 events. Figure 1.6 shows example plots of D_S for the Greek data, which were previously studied at one site from a variety of magnitudes and distances [Ktenidou et al. 2013]. Hypocentral distance effects on the *S*-wave duration may be approximated for regions such as California [W. J. Silva, *personal communication*, 2013] as follows:

$$T_{d-prop} = 0.1 \cdot R_h \text{ (sec)} \tag{1.9}$$

This expression (i.e., the empirical factor of 0.10) agrees reasonably well with the significant durations of D_{a5-75} and D_{a5-95}, for which Kempton and Stewart [2006] found factors of 0.07 and 0.15, respectively. In Figure 1.6, the solid lines correspond to a slope of 0.1, as in Equation (1.9). The intercepts of T_{d-rup} are fixed at 10 sec for **M** < 4.5 and at 15 sec for 4.5 < **M** <6.5 to illustrate the increasing trends of T_{d-prop} against R_h. The figure shows that T_{d-prop} is conservatively predicted by Equation (1.9) for this range of magnitudes.

After having fixed T_{d-prop} by Equation (1.9), we then estimated T_{d-rup} in Equation (1.8) in Step 2. Assuming Brune's [1970; 1971] ω^2 source model and Aki's [1967] scaling law hold, f_c is calculated as follows:

$$f_c = 4.9 \cdot 10^6 \beta \left(\frac{\Delta\sigma}{M_0} \right)^{\frac{1}{3}} \tag{1.10}$$

since

$$M_0 = 10^{1.5M + 16.05} \tag{1.11}$$

where β is shear-wave velocity at the source and was taken as 3.2 km/sec. $\Delta\sigma$ is the stress drop and was taken as 60 bar (6 MPa) for an average value in California [Atkinson and Silva 1997]. Using Equation (1.10), we calculated T_{d-rup} in Table 1.1 as $1/f_c$. Figure 1.7 compares the T_{d-rup} in Table 1.1 to those observed from Greek and NGA-West2 events. It shows that Table 1.1 underestimated D_S for almost all Greek and NGA-West2 events. Hence the theoretical T_{d-rup} defined as $1/f_c$ is not adequate for this study.

Based on this observation, a longer T_{d-rup} was defined for **M** < 6.5, following the results for the Greek data. For **M** > 7 events, which are greater than the Greek data magnitude range, the theoretical approach to define T_{d-rup} worked well, although it tended to slightly underestimate some durations (see Figure 1.7). The theoretical approach ($1/f_c$) also significantly underestimated one distant record of the Denali (**M**7.9) earthquake in Alaska. To avoid underestimation, a more conservative rule for large-magnitude earthquakes was chosen by assuming unilateral fault rupture (i.e., $T_{d-rup} = 2/f_c$), which is the case for the Denali earthquake (e.g., Ozacar and Beck [2003]). Table 1.2 and Figure 1.7 show T_{d-rup} after applying these adjustments.

T_{d-rup} for **M** < 6.5 is now well constrained. However, for **M** > 6.5, assuming $T_{d-rup} = 2/f_c$ led to overestimations of the overall duration except for the Denali recording. T_{d-rup} as defined in Table 1.2 also included the coda waves and very often exceeded even the entire record duration. Therefore, we modified the large-magnitude rule to $T_{d-rup} = 1/f_c$, multiplied with a constant factor of 1.4. This was an attempt to be less conservative and to include all possible later arriving significant *S*-waves, while reducing the large durations for large magnitudes. Table 1.3 shows the modified T_{d-rup} values, which are also plotted in Figure 1.7. The figure shows that these are acceptable duration estimates for magnitudes between 3.5 and 7.9. These values allow coda windows for most recordings with adequate total length, while keeping the strongest motion in the *S*-wave window.

These values are implemented into the data processing code for the automatic selection of the *S*-wave window. If, based on inspection, the analyst believes these automatically picked values to be significantly incorrect for a given record, or if the *S*-wave window is contaminated by an aftershock, then the record is flagged by the analyst for additional processing because the only modification the analyst can perform in this step is to correct an erroneous *S*-wave arrival time. An example recoding is presented at the end of this report in Figures 1.12–1.15.

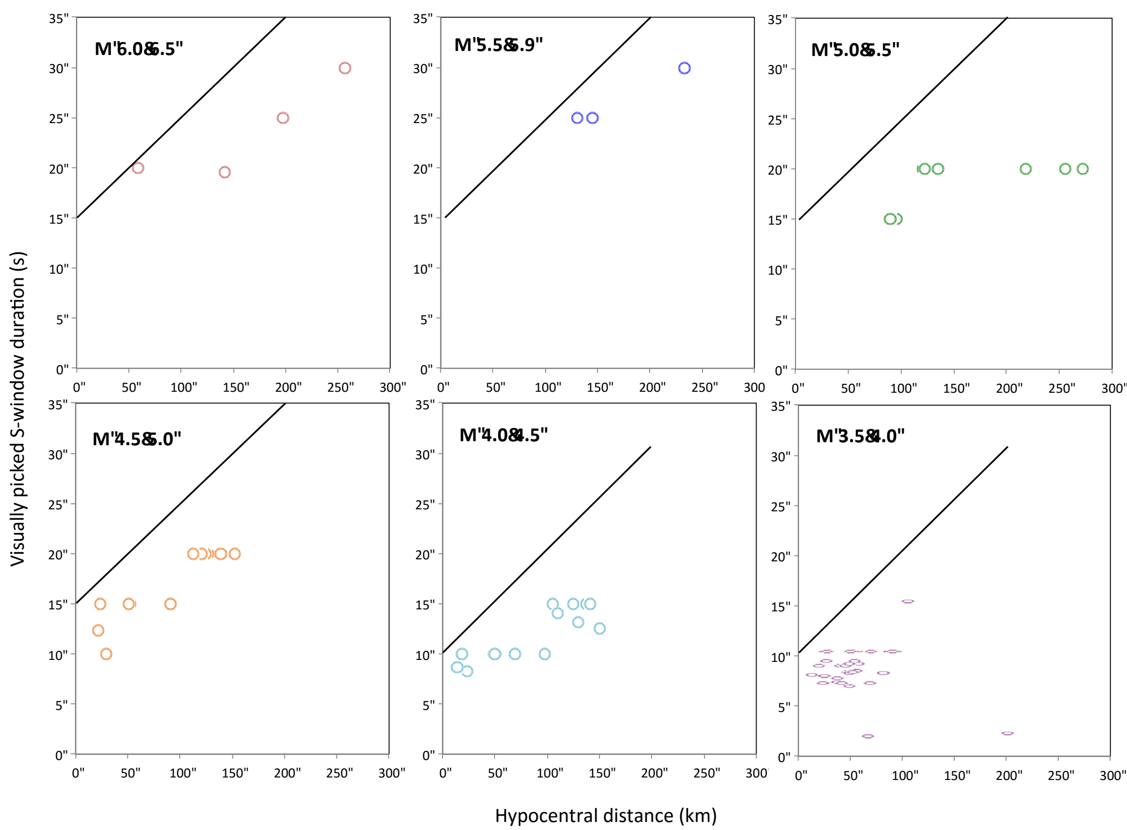

Figure 1.6 Variation in *S*-wave duration with magnitude based on visual inspection of Greek events (records and durations taken from Ktenidou et al. [2013]).

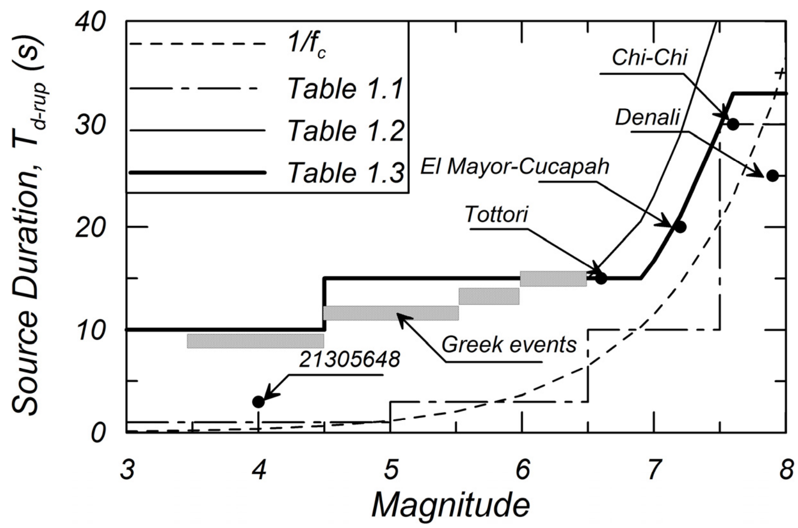

Figure 1.7 **Comparison of various schemes to predict $T_{d\text{-}rup}$ with the observed durations from data.**

Table 1.1 **Source duration versus moment magnitude based on the theoretical rupture duration.**

Magnitude (Mw)	Source duration (sec)
M < 5	1
5 < **M** < 6.5	3
6.5 < **M** < 7.5	10
7.5 < **M** < 7.9	30

Table 1.2 **Source duration versus moment magnitude after adjustments based on the NGA-West2 and Greek data.**

Magnitude (M_w)	Source duration (sec)
M < 4.5	10
4.5 < **M** < 6.5	15
6.5 < **M** < 7.9	2/fc

Table 1.3 **Recommended source duration versus moment magnitude for this study**

Magnitude (M_w)	Source duration (sec)
M < 4.5	10
4.5 ≤ **M** < 6.9	15
6.9 ≤ **M** < 7.9	1.4/fc
M ≤ 7.9	33

1.8 CODA TIME WINDOW

One definition of the onset of the coda window is twice the *S*-wave travel time after the *S*-wave arrival time [Aki 1969; Phillips and Aki 1986; and Kato et al. 1995]. This definition generally provides the directionally averaged coda wave due to backscattered waves coming from all directions. It also gives a theoretically consistent coda-wave onset. However, it may also allow *S*-waves into the coda window for cases of long source duration and short hypocentral distance. Finally, it may also exclude many records for which post-*S*-wave windows are available, but not long enough to include this delayed onset of the window, especially at long hypocentral distances.

As an alternative, the coda window onset definition is defined as beginning immediately following the *S*-wave windows [Novelo-Casanova and Lee 1991; Wong et al. 2001]. This definition maximizes the number of coda windows available from the dataset, although some of these records may contain late arriving *S*- and/or surface waves. Further discussion on this issue includes Padhy et al. [2011], who discussed the various assumptions made in literature for the coda onset, and Satoh et al. [2001], who presented a comparison between early and late coda onsets.

For this project, which had the goal of obtaining as many FAS from coda windows as possible, a new approach was devised. In this approach, the end of the coda window is defined to make use of as much of the record as is available. Information is provided to the user as to the quality of coda onset; by distinguishing between the different definitions, the user can select which coda windows to use for their analyses.

The end of the coda window is generally defined as the end of the record. However, given that a few records have unusually long durations, we compared the actual end-of-record time (t_{end}) with an artificial end-of-record time ($t_{end} = t_S + 3D_S$) to avoid choosing the coda window at the end of these time histories, since the window will then probably be dominated by the least significant ground motion. Hence, the end of the coda window is defined as the minimum of these two values:

$$t_c^f = \min\left(t_{end}, t_S + 3 \cdot D_S\right) \tag{1.12}$$

The coda window length (D_c) is simply chosen to be the same as D_S if possible. When this window length is unavailable (i.e., due to overlap with the *S*-wave window), then the D_c is the remaining duration between t_S^f and t_c^f. Hence, the start time of the coda window (t_c) is taken to be:

$$t_c = \max\left(t_S^f,\ t_c^f - D_S\right) \tag{1.13}$$

and the duration of the coda window is then less than the *S*-wave duration and given by:

$$D_c = t_c^f - t_c \le D_S \tag{1.14}$$

We examined these window definitions on several records and confirmed that they work well except in those cases where coda windows included *S*-waves. Such windows were flagged by the analysts for further review.

The processing code automatically flags the record in two cases, depending on the location of the coda window in the time series. In the first case, the code compares t_c with the theoretical value for the coda window onset ($t_{theo} = t_S + 2R_h/\beta$). If $t_c \leq t_{theo}$, a flag is added; this will be included in the final flatfile so that users can choose the definition for the coda window. This flag does not lead to reprocessing by an experienced analyst, but it is provided to assist the data user in case they wish to exclude coda windows that do not comply with the theoretical coda onset definition. Figure 1.8 shows some examples of coda windows. In Figure 1.8(a), the coda window starts near the theoretical [Aki 1969] coda arrival, whereas in Figure 1.8(b), it starts at a later time. In Figure 1.8(c), the window starts before the theoretical arrival due to the limited record length. These different coda window onsets are flagged by the following equation and are shown in Figure 1.8.

$$\text{flag} = \begin{cases} 1, & t_c \leq t_{theo} \\ 0, & \text{otherwise} \end{cases} \tag{1.15}$$

In the second case, a check for possibly inadequate (short) coda window durations is performed. A coda window has a length of $D_c \leq D_S$, but that duration may not provide adequate spectral resolution, especially considering the standard PEER processing [Ancheta et al. 2013] cosine tapering at the end of the entire record. The taper at the end of the record is 5% of the entire record duration (e.g., 2 sec for a 40 sec-long record and 15 sec for a 300 sec-long record). Since the percentage is a constant, we can check D_c against the taper duration ($D_{tap} = 0.05t_{end}$). We require that the taper duration is not greater than 30% of the coda window length (i.e., $D_c \geq D_{tap}/0.3 = 0.17 \cdot t_{end}$), and that the coda window length is greater than 10 sec. If these conditions are not satisfied, then the record is flagged as having possibly inadequate coda duration, and it is reprocessed by an experienced analyst. Figure 1.9 shows an example recording for the coda window. Based on the following classification scheme, the recording was flagged as 1 sec during the data processing.

$$\text{flag} = \begin{cases} -999, & \text{no coda window} \\ 1, & D_c < 10 \mid D_c < 0.17 \cdot t_{end} \\ 0, & \text{otherwise} \end{cases} \tag{1.16}$$

The automatic selection of the coda window cannot be altered by the analyst. If the analyst believes these automated values to be incorrect, or if the coda-wave window contains an aftershock, the record is flagged for further processing. Figure 1.10 shows an example recording that includes a small aftershock in the coda window. The flagged records are then further reviewed by experienced analysts.

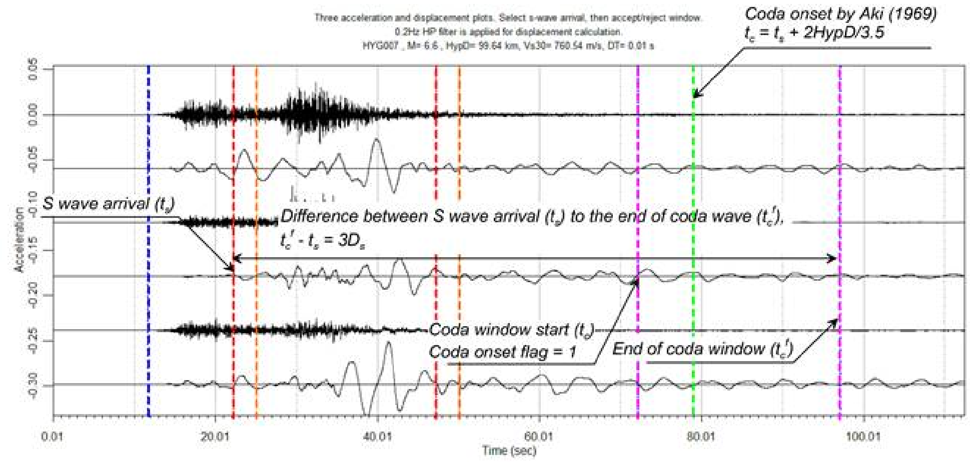

(a)

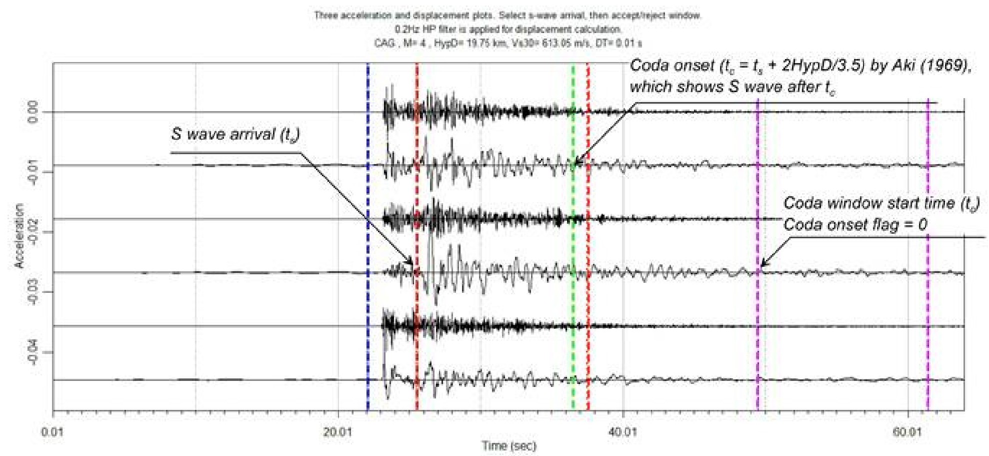

(b)

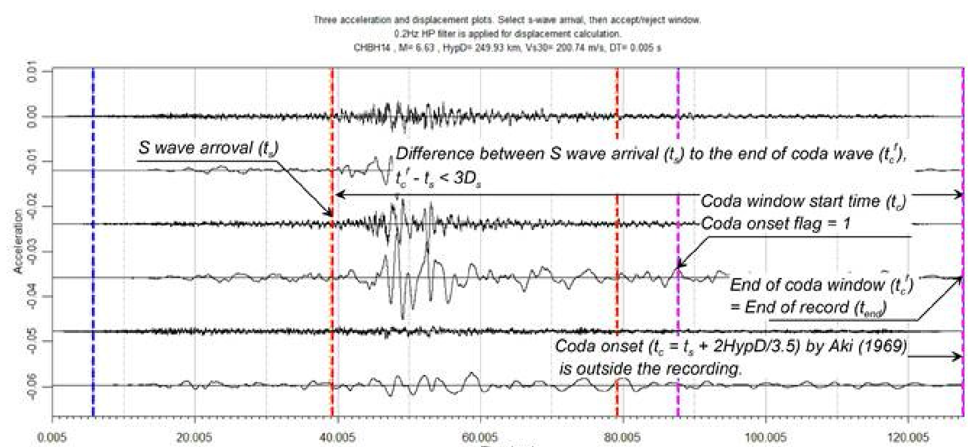

(c)

Figure 1.8 **Coda window starts (a) near, (b) after, and (c) earlier than the theoretical [Aki 1969] coda arrival time.**

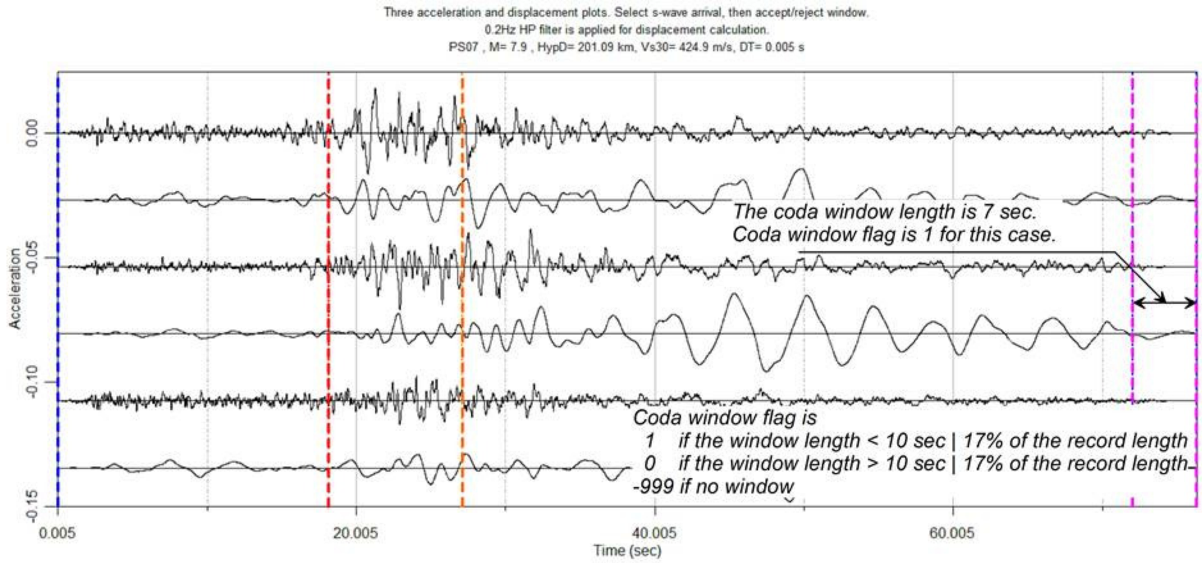

Figure 1.9 Example of the automatic computation of the coda window duration and flag.

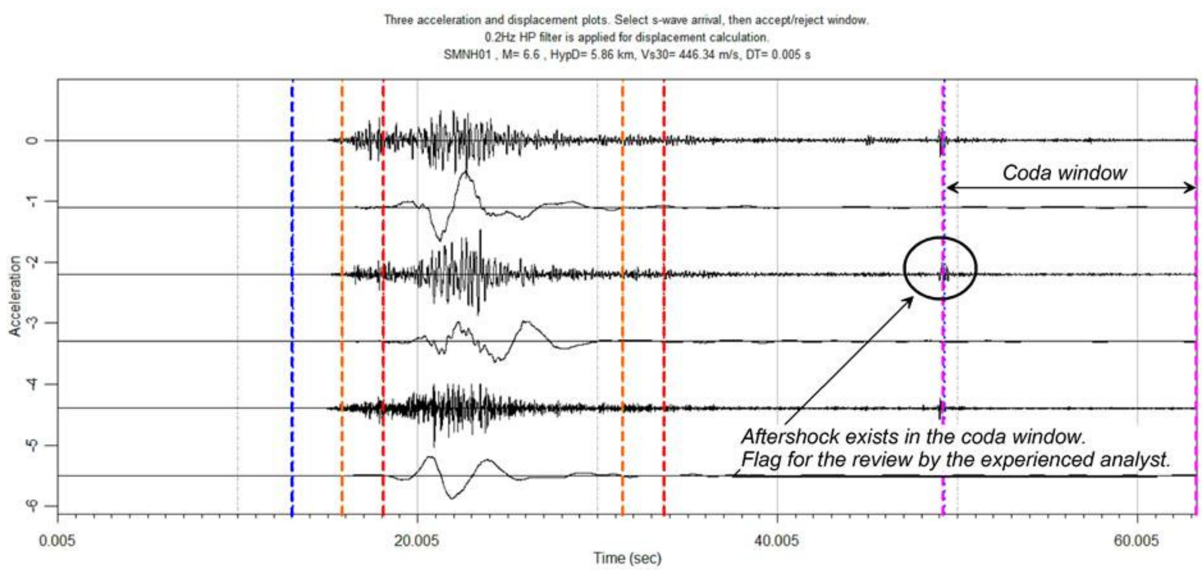

Figure 1.10 User-defined flag if the *S*- or coda window is problematic, e.g., contains an aftershock.

1.9 FLAGGED RECORDS

Most flagged records are reviewed and reprocessed by experienced analysts, with the exception of late *S*-wave triggers (which are reviewed to confirm before rejection from further processing) and late coda onsets (which are accepted). Information from the flags, such as late *P*/*S* triggers, short-noise/coda windows, coda-waves onsets that do not follow the theoretical onset rule of Aki [1969], and various other issues (e.g., aftershocks), can then be included in the FAS flatfile. Table 1.4 summarizes all of the flags during data processing.

Table1.4. Types of flagged records during data processing.

Name	Type	Result
Late *S*-wave trigger	User	Rejection (after confirmation)
Late *P*-wave trigger	Auto (criterion: $\Delta t_{S-P} \geq 30\% \cdot R_h / 8$)	Review
Short noise window	Auto (criterion: $t_P \leq 10$ sec)	Review
Short coda window	Auto (criteria: $D_c \leq 10$ sec or $D_c \leq 0.17 t_{end}$ $a' = a = \overline{a}$ $df = 1/D_{tot}$ $df(k-1)$ dt $x(j)$)	Review
Coda onset prior to 2* *S*-wave travel time	Auto (criterion: $t_c \leq t_{theo}$)	- (for info only)
Coda contaminated with *S*-waves; aftershock in *S*-wave or coda window; contamination in noise	User	Review

1.10 *DC* (MEAN) REMOVAL, TAPERS, ZERO PADDING, AND FAS COMPUTATION

1.10.1 *DC* (Mean) Removal and Tapers

Before calculation of the FAS, the various windowed time series are processed in the time domain for D_C removal as defined by the following equation:

$$a' = a = \overline{a} \tag{1.17}$$

where a' denotes the acceleration time series after D_C removal. a and $\overline{a}$ denote the windowed acceleration time series and the mean offset value, respectively. Cosine tapers are then applied to the beginning and end of each time window. Table 1.5 lists the length of cosine tapers applied to the acceleration series: recall that in most cases the entire time history has already been tapered with 1% and 5% at beginnings and ends.

Table 1.5 Cosine taper length applied to windowed accelerations.

Windowed time histories	Cosine taper length	
	Start time	**End time**
Entire record	1% of total length	1% of total length
Pre-event noise	0.5 sec	0.5 sec
P-wave window	0.5 sec	0.5 sec
S-wave window	0.5 sec	0.5 sec
Coda-wave window	0.5 sec	0.5 sec

1.10.2 Zero Padding and Fourier Spectra

Following tapering and then D_C (mean) removal, a series of zeros is added to the end of the records. A common duration (D_{tot}) is chosen for all windows in the dataset, so that the resulting FAS have a common frequency step ($df = 1/D_{tot}$). This is convenient for users for two reasons:

- A common df for the different time windows of each record (*P*-, *S*-, coda, and noise) facilitates the computation of SNR, which is a check often performed before choosing the useable frequency range of the data.
- If a user wishes to process a large number of data, providing a common df facilitates statistical calculations at chosen frequency values. One need only select frequencies without interpolation of the data near the required value. This process maintains the variance of the signal and should facilitate future analyses.

In order to decide on the value of D_{tot}, we sorted all the records in the NGA-West2 flatfile based on the time step (dt), and listed the longest recordings for the different time steps. Table 1.6 shows the longest recordings for time steps of 0.0025, 0.0050, 0.0100, and 0.0200 sec, respectively. These time steps represent 91% of NGA-West2 database. The longest duration in the flatfile is 1010 sec (Table 1.6), which was recorded at Shenxian Station from the Wenchuan earthquake. Nearly all (91%) of the recordings will be padded by a series of zeros at the end, to a D_{tot} of 1,310.72 sec, which is a common power of two for these dt values. This process creates a consistent df of 0.000763 Hz.

However, some recordings (9%) do not have the instrument sampling dt as a multiple of 0.0025 sec. For example, many recordings of the Kocaeli, Turkey, earthquake, have a dt of 0.0078 sec. When the recording has a different time step from those listed in Table 1.6, the duration is selected as a power of two multiplied with the time step that creates the closest duration possible to 1310.72 sec, but shorter. This algorithm is expressed by the following equation:

$$D_{tot} = 2^K dt \tag{1.18}$$

where

$$K = \text{floor}\left[\log_2\left(1310.72/dt\right)\right] \tag{1.19}$$

For example, if the dt is 0.0078 sec, K is calculated to be 17, hence D_{tot} becomes 1,022.3616 sec. This D_{tot} is consistent for these recordings but requires additional interpolation if FAS values are compared to other recordings; note that the recordings with different time steps are only 9% of total database.

By using the windowed time series after D_C removal, tapering, and zero adding, FAS and Fourier Phase Spectra (FPS) are computed as follows:

$$FAS_k = T\left|C_k\right| \tag{1.20}$$

where

$$C_k = \frac{1}{N}\sum_{j=1}^{N} x(j)\omega_N^{(j-1)(k-1)} \tag{1.21}$$

$$\omega_N = e^{(-2\pi i)/N} \tag{1.22}$$

$$T = Ndt \tag{1.23}$$

C_k is the Fourier coefficient for each frequency $df(k-1)$, where df is the frequency step. The term $x(j)$ represents a time series, N represents the number of data points in the time series, and dt is the time step of the series. The FPS is calculated from the real and imaginary values of Fourier spectra as follows:

$$FPS = \tan^{-1}\left[\text{Im}\left(C\right)/\text{Re}\left(C\right)\right] \tag{1.24}$$

where the phase ranges from $-\pi$ to π in the output. The FAS flatfile will be populated following the smoothing and de-sampling procedures used in the NGA-East project [Goulet et al. 2014]. Figure 1.11 shows an example of the computed and smoothed FAS for all time windows, using the example record of Figure 1.1. The FAS in the figure have units of *g*'s and have been smoothed to show the trends at high frequencies.

The current NGA-West2 flatfile does not until now include metadata columns with the sampling rate of each instrument or the total number of data points of each record. This is because up to now the focus of the NGA projects has been to provide users with response spectral values. In the framework of the current project, which aims at providing users with time series and FAS, columns with sampling rates and numbers of points will be added to the FAS flatfile.

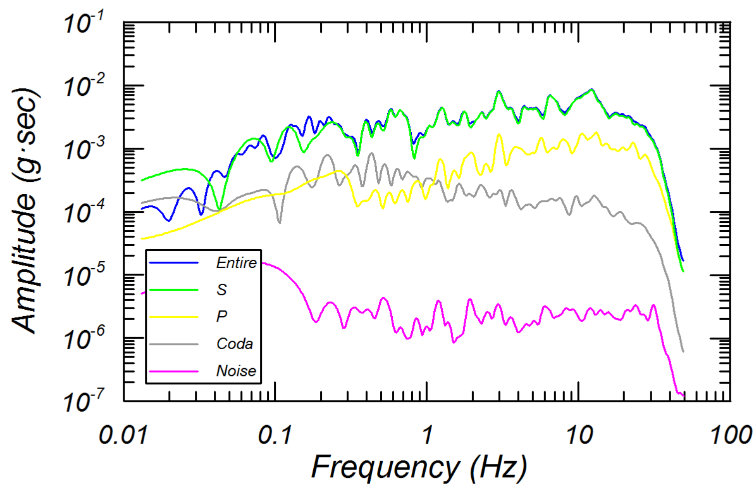

Figure 1.11 **Computed FAS for all time windows shown in the example record of Figure 1.1 (Tottori earthquake, station HYG007).**

Table 1.6 **Common duration for FAS calculation (covers 91% of the total number of records).**

***dt* (sec)**	**RSN for longest recordings**	**Number of points**	**Duration (sec)**	**Duration after zero padding (sec)**	**Power**	***df* (Hz)**
0.0025	495	4113	10.2825	1310.72	19	0.000762939
0.005	4620	202001	1010.005	1310.72	18	0.000762939
0.01	4614	60001	600.01	1310.72	17	0.000762939
0.02	8152	7500	150	1310.72	16	0.000762939

1.11 FREQUENCY RANGE LIMITATIONS AND CONSIDERATIONS

Finally, we emphasize that, although FAS are computed up to each record's Nyquist frequency, this does not mean that a spectrum is usable within the entire frequency range. The user should consult the flatfile for the high-pass frequency for each horizontal component (values HP-H1, HP-H2, columns DT-DU) and low-pass frequency (LP-H1, LP-H2 values, columns DV-DW) depending on the filtering performed on the traces. The recommended minimum and maximum usable frequencies are determined from a previous study by Abrahamson and Silva [1997], and are calculated by the following expressions taking into account both components, H1 and H2:

$$\text{Lowest Usable Frequency (LUF)} = 1.25 \cdot \max(\text{HP-H1, HP-H2}) \quad (1.25)$$

$$\text{Highest Usable Frequency (HUF)} = \min(\text{LP-H1, LP-H2})/1.25 \quad (1.26)$$

A second caution is that these filters were based on noise in the entire record and are only strictly applicable to the entire record spectrum (see Figure 1.11). Shorter time windows may have increased levels of noise in the spectrum. Additionally, the user should note those cases in the flatfile that contain zero values for LP-H1, LP-H2; zero indicates that the filtering was performed prior to PEER acquiring the data; generally, this is Volume II data when the unprocessed (Volume I) data were not available. In these cases, the user should assess the usable frequencies for those records through visual inspection of the FAS.

The user will also notice that window lengths (e.g., pre-event noise window) are sometimes shorter than 1/LUF. In that case, the FAS at periods longer than the window length are generated by adding a series of zeros at the end of the windows. Therefore, in such cases, the lowest usable frequency is 1/(window length) rather than the LUF defined by Equation (1.25). Finally, the data recorded by the KiK-net and K-Net arrays in Japan have an instrument response modified by an anti-alias filter that exhibits decay similar to a three-pole Butterworth filter with a corner frequency of 30 Hz [Aoi et al. 2004]. The user should consider that, regardless of the filters mentioned in the flatfile, these records have a maximum usable frequency of about 30/1.25 = 24 Hz, due to the anti-alias filter incorporated in the data acquisition system. This is of great importance if such records are used to compute high-frequency parameters such as κ (Ktenidou et al., 2014).

1.12 EXAMINING THE PROPOSED METHOD FOR DIFFERENT HYPOCENTRAL DISTANCES

Example records were processed for a range of regions, magnitudes, and distances, to test the proposed methodology using NGA-West2 data. The selected recordings are from the following earthquakes: 21305648 California earthquake, 09/06/2003 (**M**4.0), Tottori, Japan, 10/16/2000 (**M**6.6), El Mayor-Cucapah, Mexico, 4/4/2010 (**M**7.2), and Denali, Alaska, 11/03/2002 (**M**7.9). Tables 1.7–1.10 list the processed records. The hypocentral distances range from 5 to 500 km, in order to examine the windowing procedure proposed in this study. Figures 1.12–1.15 show the selected time windows for all four earthquakes. These figures demonstrate that obtaining the complete set of all five time windows (noise, *P*-wave, *S*-wave, coda, and the entire record) becomes difficult as magnitude increases. This is expected, because for larger-magnitude recordings, the recording generally does not include significant pre-event or coda windows. In addition, nearly all large-magnitude recordings in NGA-West2 have shorter lengths due to a variety of factors, including analog recording systems, trigger levels, pre-event memory length, and total record length criteria established by the strong-motion networks (e.g., GGS\CSMIP and UGSS\NSMP). In contrast, the small-to-moderate California dataset was generally obtained from continuously recording seismic networks (e.g., CIT\SCSN, BDSN, and the USGS). Therefore, these recordings generally have significantly longer pre-event and post-event lengths because these lengths were requested by PEER from the data network providers. Hence, the FAS can also be calculated for the pre-event and coda windows for these data. In summary, the proposed window selection method works well for this range of recordings.

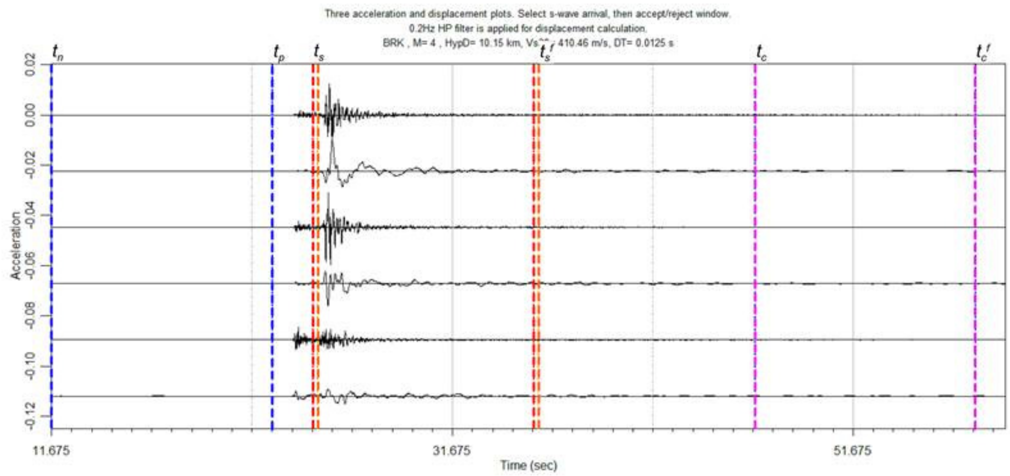
Three acceleration and displacement plots. Select s-wave arrival, then accept/reject window.
0.2Hz HP filter is applied for displacement calculation.
Acceleration
Time (sec)
11.675
31.675
51.675

(a)

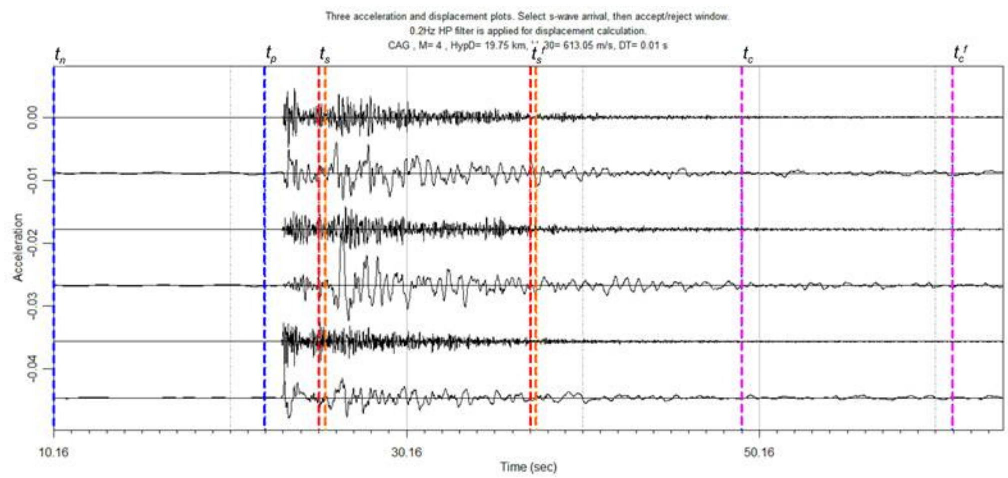
Three acceleration and displacement plots. Select s-wave arrival, then accept/reject window.
0.2Hz HP filter is applied for displacement calculation.
Acceleration
Time (sec)
10.16
30.16
50.16

(b)

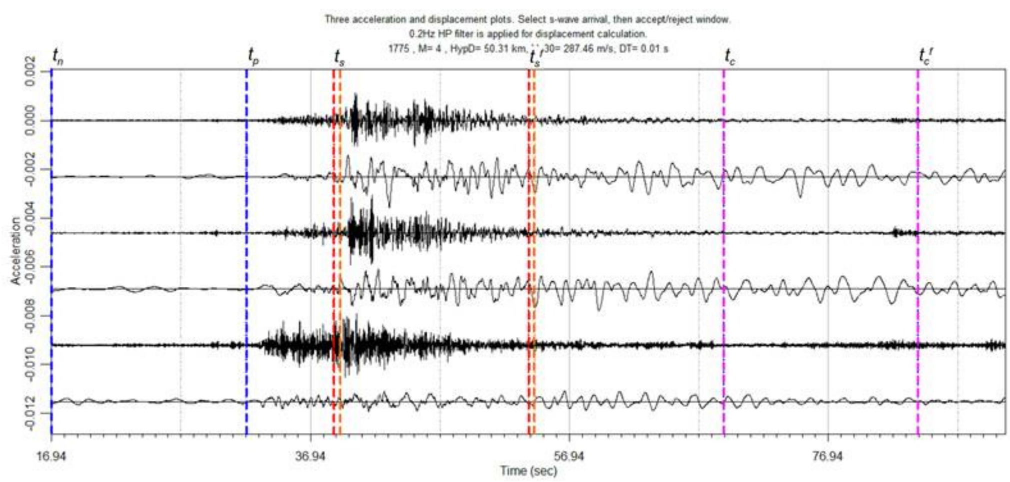
Three acceleration and displacement plots. Select s-wave arrival, then accept/reject window.
0.2Hz HP filter is applied for displacement calculation.
Acceleration
Time (sec)
16.94
36.94
56.94
76.94

(c)

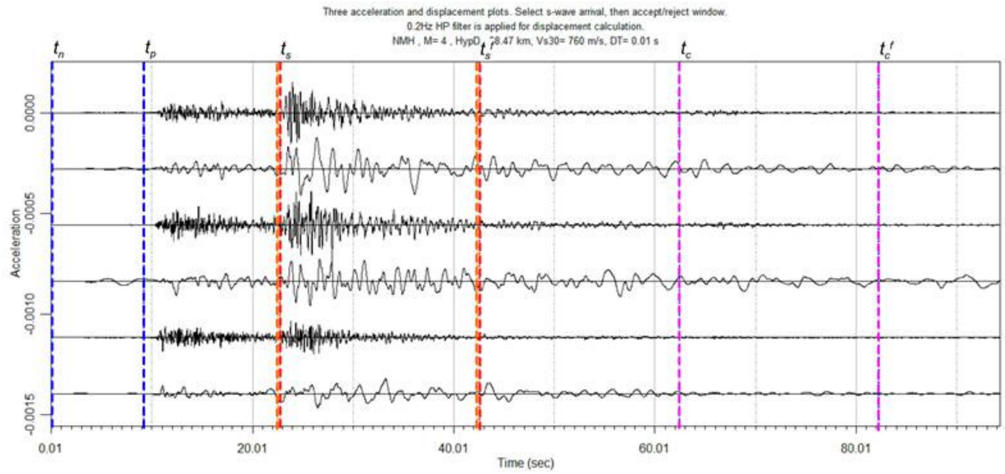

(d)

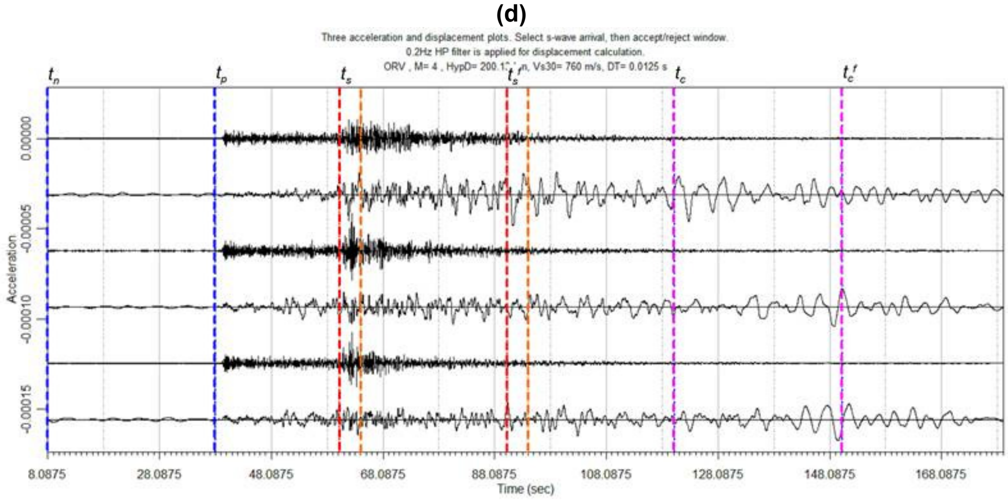

(e)

Figure 1.12 **The automatic choice of windows (after manual *P* and *S* onset selections) for a series of records of the 21305648 California earthquake at: (a) Haviland Hall, U.C. Berkeley, 10 km, (b) Angel Island, 20 km, (c) Mountain View; Fire Station 3, 50 km, (d) Mt. St. Helens, 100 km, and (e) Oroville Dam, Oroville, 200 km.**

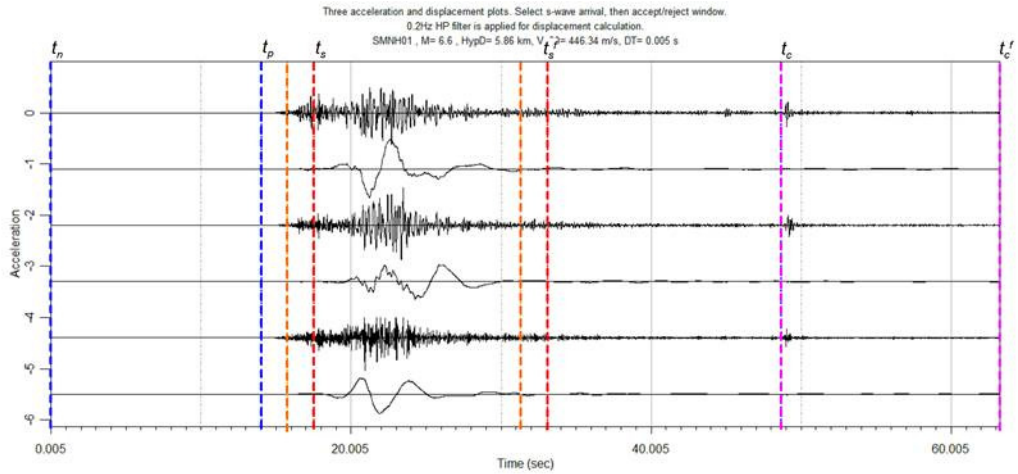
Three acceleration and displacement plots. Select s-wave arrival, then accept/reject window.
0.2Hz HP filter is applied for displacement calculation.
SMNH01 , M= 6.6 , HypD= 5.86 km, Vs30= 446.34 m/s, DT= 0.005 s
Acceleration
Time (sec)

(a)

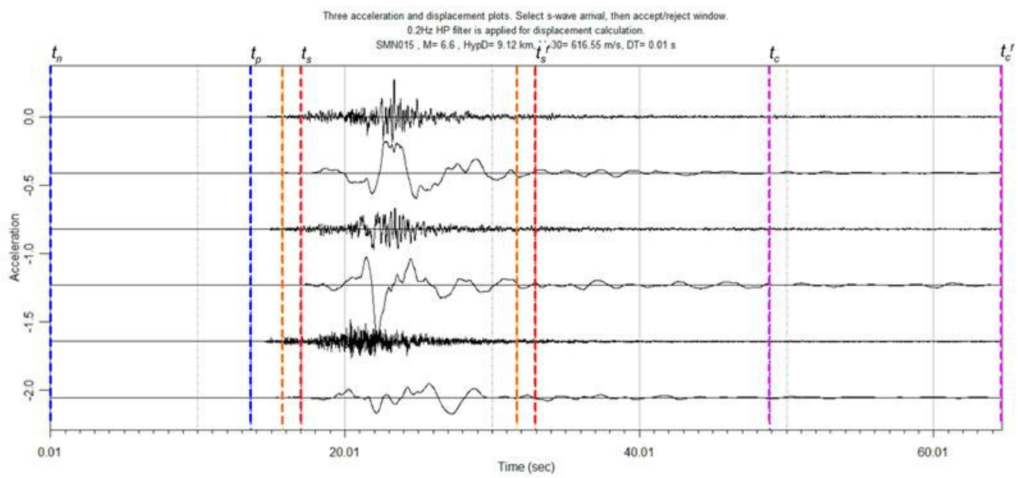
Three acceleration and displacement plots. Select s-wave arrival, then accept/reject window.
0.2Hz HP filter is applied for displacement calculation.
SMN015 , M= 6.6 , HypD= 9.12 km, Vs30= 616.55 m/s, DT= 0.01 s
Acceleration
Time (sec)

(b)

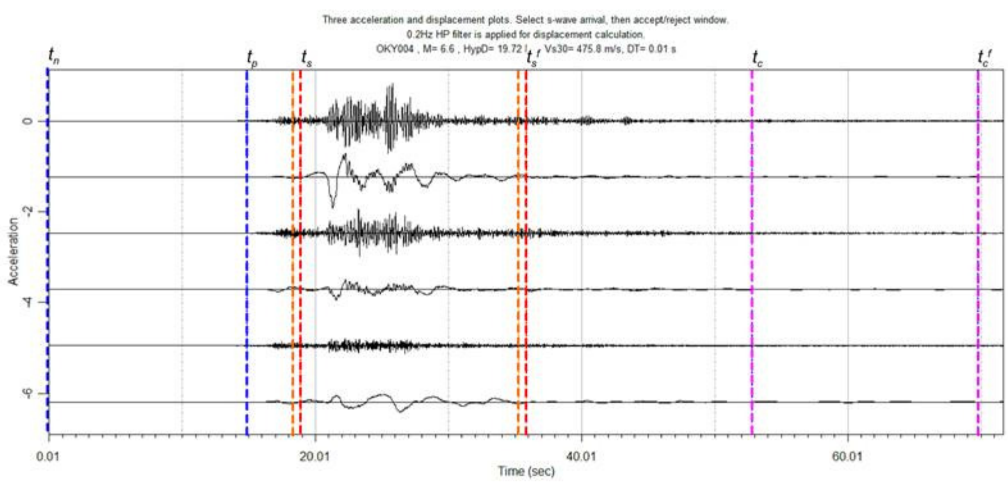
Three acceleration and displacement plots. Select s-wave arrival, then accept/reject window.
0.2Hz HP filter is applied for displacement calculation.
OKY004 , M= 6.6 , HypD= 19.72 km, Vs30= 475.8 m/s, DT= 0.01 s
Acceleration
Time (sec)

(c)

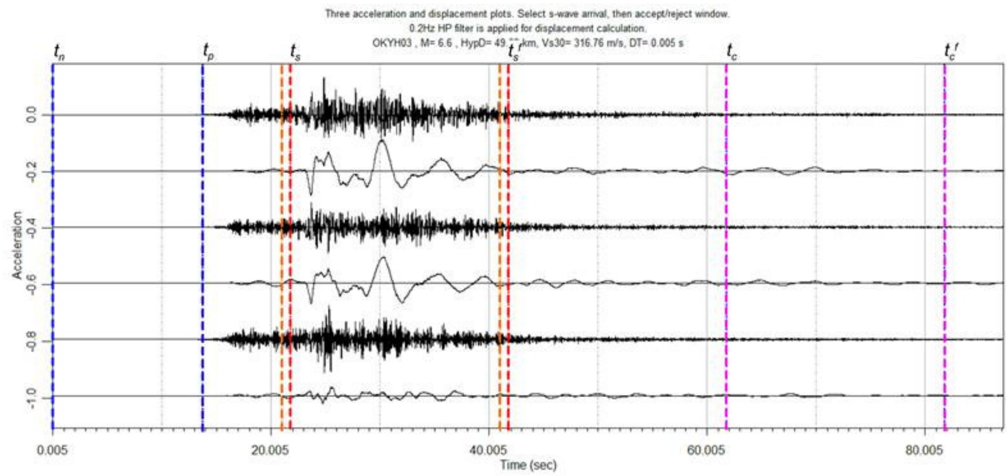

(d)

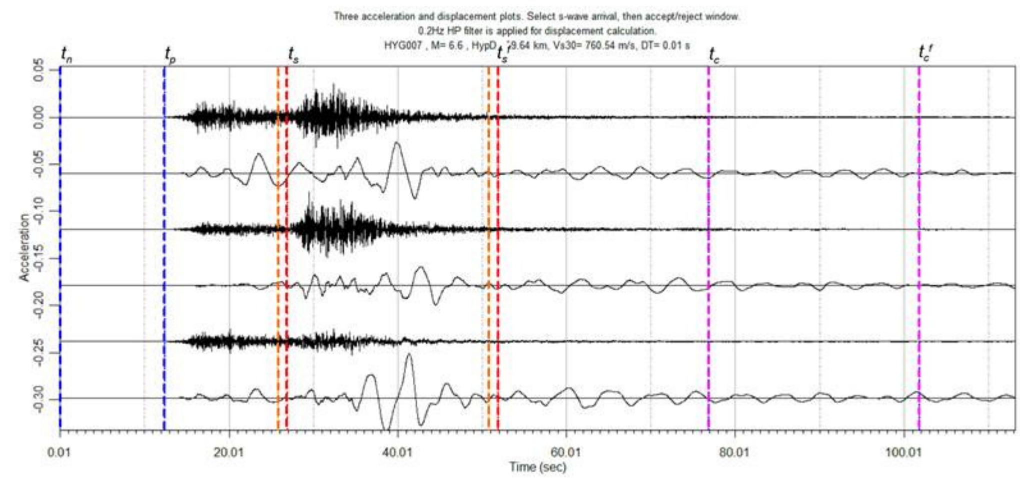

(e)

Figure 1.13 **The automatic choice of windows (after manual *P* and *S* onset selections) for a series of records of the Tottori, Japan, earthquake at (a) SMNH01, 6 km, (b) SMN015, 9 km, (c) OKY004, 20 km, (d) OKYH03, 50 km, and (e) HYG007, 100 km.**

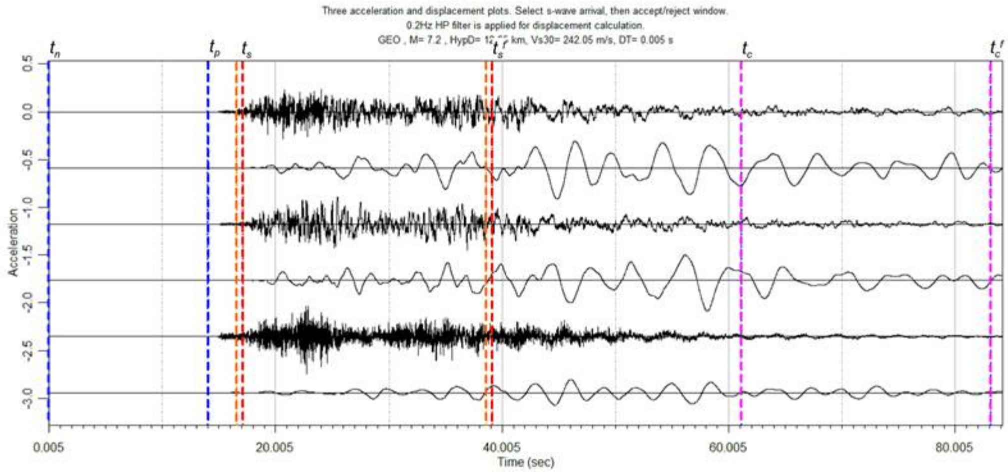
Three acceleration and displacement plots. Select s-wave arrival, then accept/reject window.
0.2Hz HP filter is applied for displacement calculation.
GEO , M= 7.2 , HypD=
km, Vs30= 242.05 m/s, DT= 0.005 s
t_n
t_p
t_s
t_s^f
t_c
t_c^f
Acceleration
0.5
0.0
-0.5
-1.0
-1.5
-2.0
-2.5
-3.0
0.005
20.005
40.005
60.005
80.005
Time (sec)

(a)

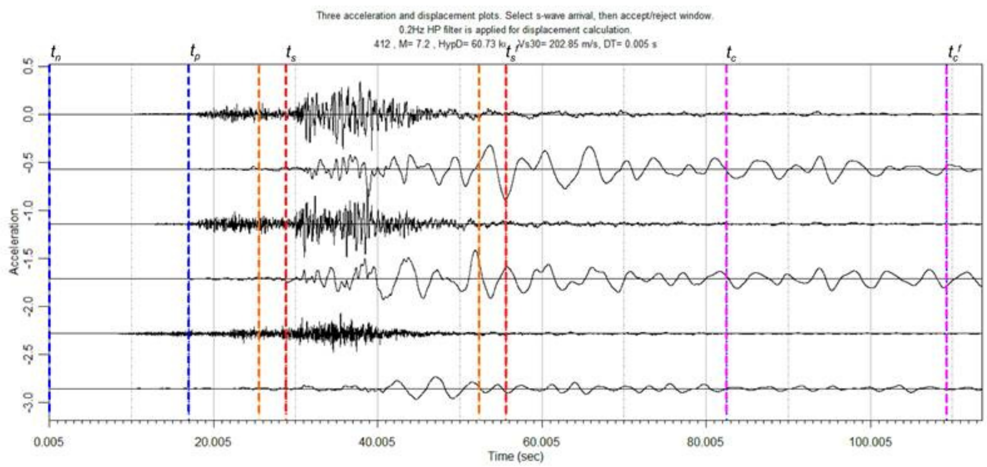
Three acceleration and displacement plots. Select s-wave arrival, then accept/reject window.
0.2Hz HP filter is applied for displacement calculation.
412 , M= 7.2 , HypD= 60.73
Vs30= 202.85 m/s, DT= 0.005 s
t_n
t_p
t_s
t_s^f
t_c
t_c^f
Acceleration
0.5
0.0
-0.5
-1.0
-1.5
-2.0
-2.5
-3.0
0.005
20.005
40.005
60.005
80.005
100.005
Time (sec)

(b)

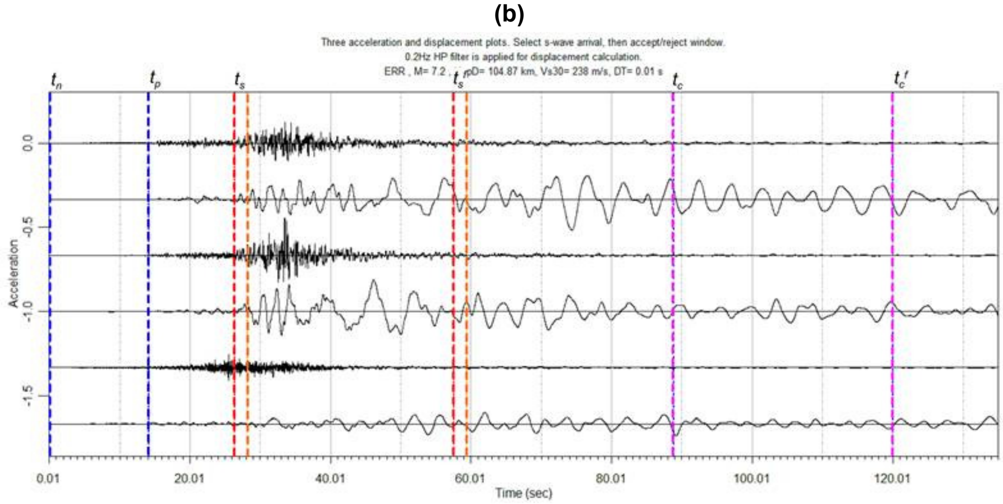
Three acceleration and displacement plots. Select s-wave arrival, then accept/reject window.
0.2Hz HP filter is applied for displacement calculation.
ERR , M= 7.2 ,
pD= 104.87 km, Vs30= 238 m/s, DT= 0.01 s
t_n
t_p
t_s
t_s^f
t_c
t_c^f
Acceleration
0.0
-0.5
-1.0
-1.5
0.01
20.01
40.01
60.01
80.01
100.01
120.01
Time (sec)

(c)

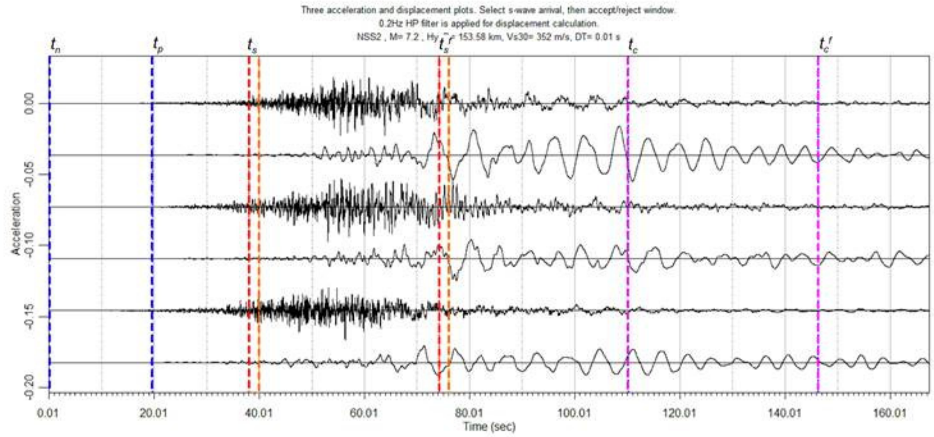

(d)

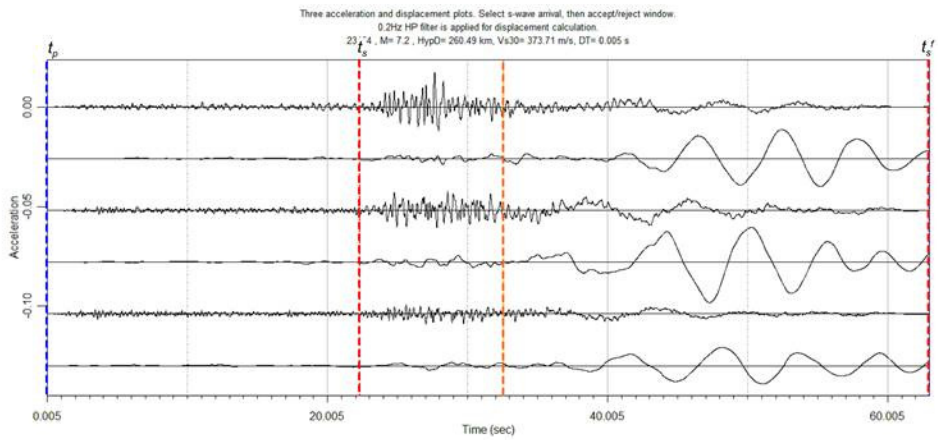

(e)

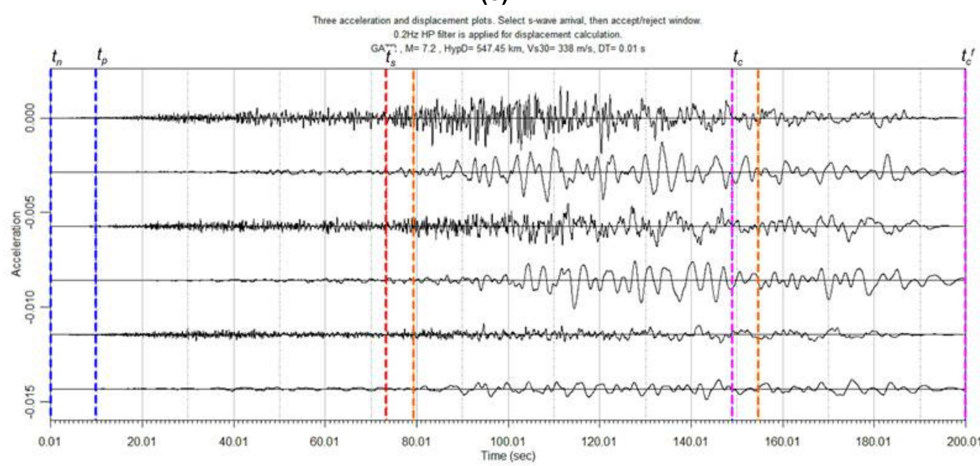

(f)

Figure 1.14 The automatic choice of windows (after manual *P* and *S* onset selections) for a series of records of the El Mayor-Cucapah, Mexico, earthquake at: (a) Cerro Prieto Geothermal, 10 km, (b) El Centro Array #10, 20 km, (c) Elmore's Ranch, 50 km, (d) North Shore Salton Sea 2, 100 km, (e) Redlands - Garden & Mariposa, 200 km, and (f) Ground to Air Transmit and Receive Compound, 490 km.

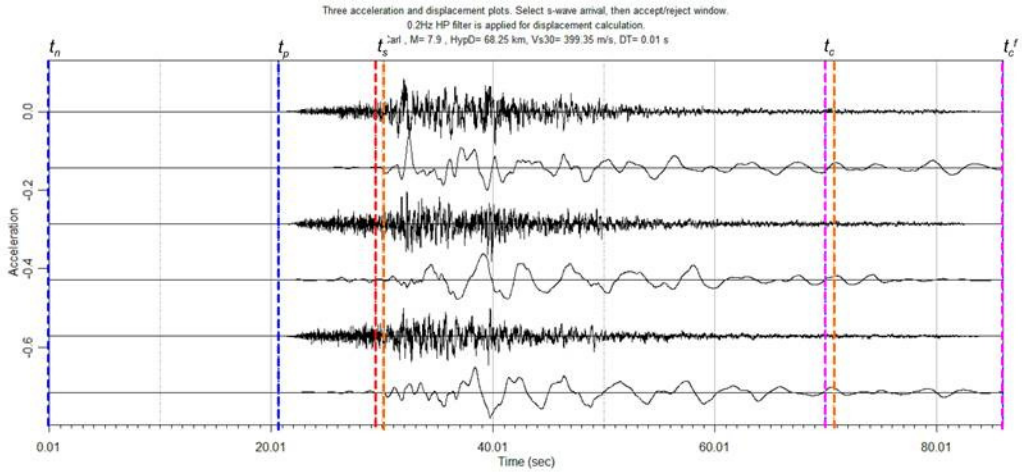
Three acceleration and displacement plots. Select s-wave arrival, then accept/reject window.
0.2Hz HP filter is applied for displacement calculation.
t_n
t_p
t_s
t_c
t_c^f
Acceleration
Time (sec)

(a)

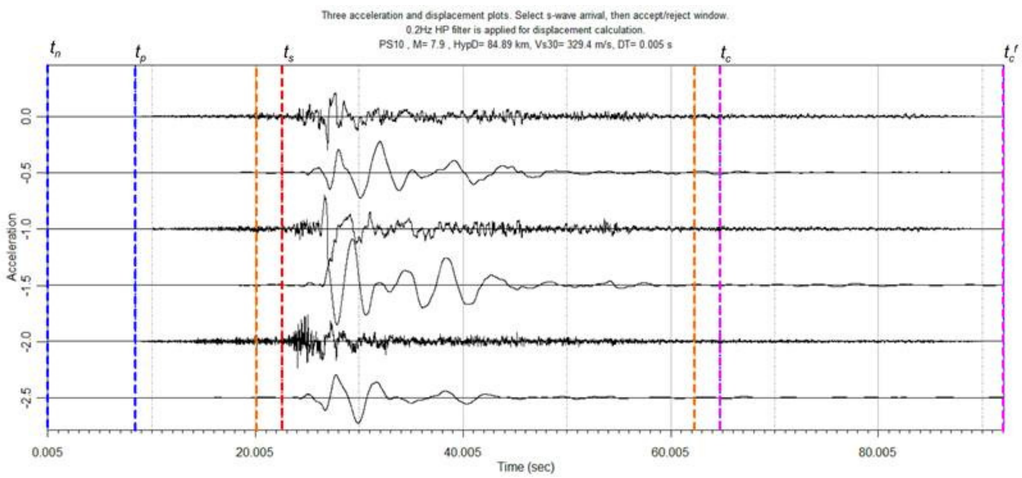
Three acceleration and displacement plots. Select s-wave arrival, then accept/reject window.
0.2Hz HP filter is applied for displacement calculation.
PS10 , M= 7.9 , HypD= 84.89 km, Vs30= 329.4 m/s, DT= 0.005 s
t_n
t_p
t_s
t_c
t_c^f
Acceleration
Time (sec)

(b)

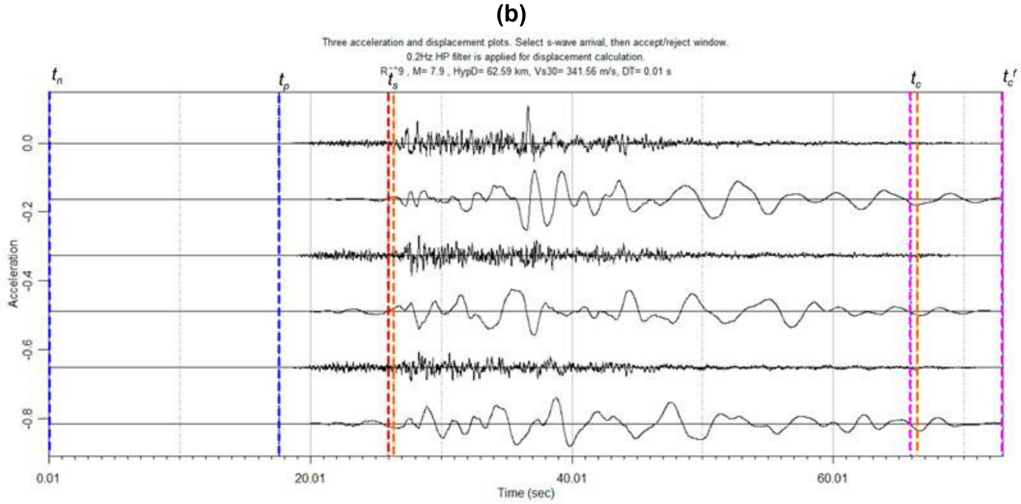
Three acceleration and displacement plots. Select s-wave arrival, then accept/reject window.
0.2Hz HP filter is applied for displacement calculation.
t_n
t_p
t_s
t_c
t_c^f
Acceleration
Time (sec)

(c)

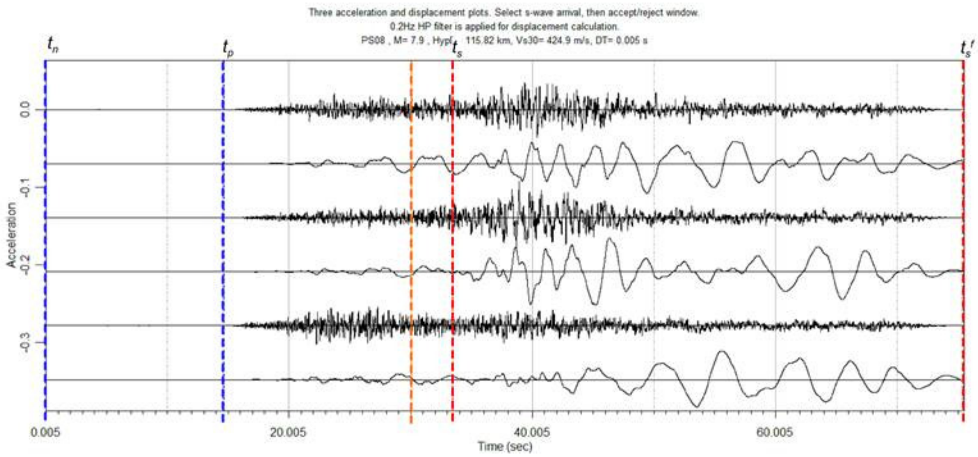

(d)

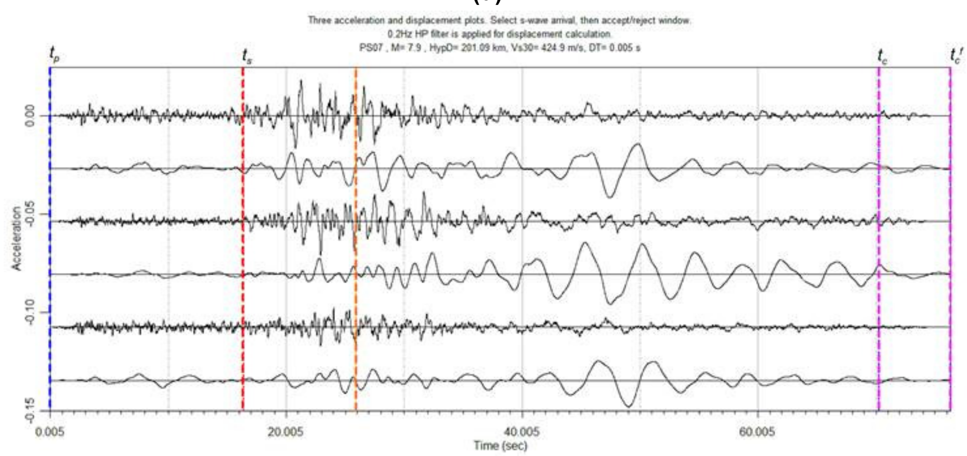

(e)

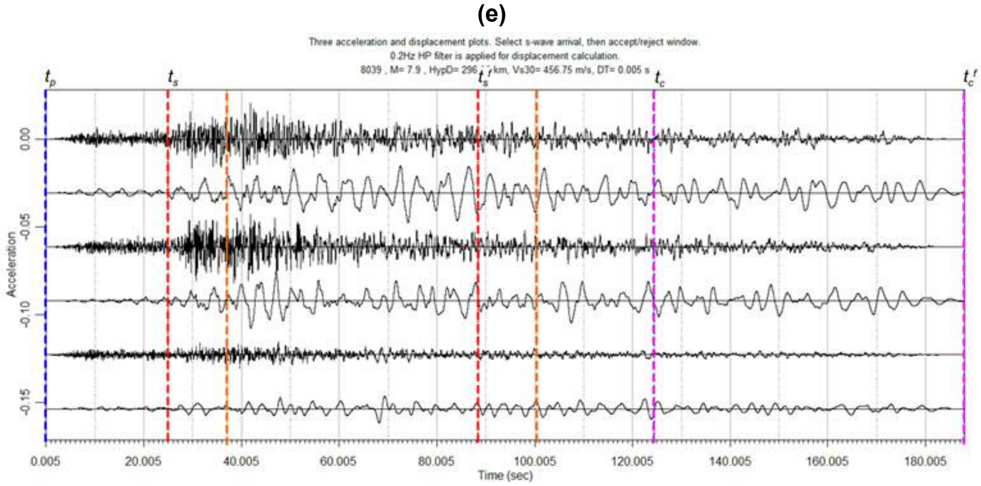

(f)

Figure 1.15 **The automatic choice of windows (after manual *P* and *S* onset selections) for a series of records of the Denali, Alaska, earthquake at: (a) Carlo, 70 km, (b) PS#10, 85 km, (c) R109, 60 km, (d) PS#08, 115 km, (e) PS#07, 200 km, and (f) 8039, 297 km.**

Table 1.7 Records used for 21305648 California earthquake, 09/06/2003 (M4.0)

RSN	Hypocentral distance (km)	Station name	File name
13046	10.15	Haviland Hall, U.C. Berkeley	BKBRKHLN.AT2 BKBRKHLE.AT2 BKBRKHLZ.AT2
13002	19.75	Angel Island	NCCAGHNN.AT2 NCCAGHNE.AT2 NCCAGHNZ.AT2
19595	50.31	Mountain View; Fire Station 3 North Rengstorff Ave; one-story; ground level	1775HNN.AT2 1775HNE.AT2 1775HNZ.AT2
19622	98.47	Mt. St. Helens	NMHHNN.AT2 NMHHNE.AT2 NMHHNZ.AT2
19584	200.13	Oroville Dam, Oroville	ORVHHN.AT2 ORVHHE.AT2 ORVHHZ.AT2

Table 1.8 Records used for Tottori, Japan, earthquake, 10/16/2000 (M6.6).

RSN	Hypocentral distance (km)	Station name	File name
3947	5.86	SMNH01	SMNH01NS.AT2 SMNH01EW.AT2 SMNH01UD.AT2
3943	9.12	SMN015	SMN015NS.AT2 SMN015EW.AT2 SMN015UD.AT2
3907	19.72	OKY004	OKY004NS.AT2 OKY004EW.AT2 OKY004UD.AT2
3921	49.82	OKYH03	OKYH03NS.AT2 OKYH03EW.AT2 OKYH03UD.AT2
3895	99.64	HYG007	HYG007NS.AT2 HYG007EW.AT2 HYG007UD.AT2

Table 1.9 Records used for El Mayor-Cucapah, Mexico, earthquake, 4/4/2010 (M7.2).

RSN	Hypocentral distance (km)	Station name	File name
5825	12.65	Cerro Prieto Geothermal	GEO000.AT2 GEO090.AT2 GEO--V.AT2
5991	60.73	El Centro Array #10	E10320.AT2 E10230.AT2 E10-UP.AT2
8522	104.87	Elmore's Ranch	CIERRHNN.AT2 CIERRHNE.AT2 CIERRHNZ.AT2
6025	153.58	North Shore Salton Sea 2	NSS2360.AT2 NSS2-90.AT2 NSS2-UP.AT2
5949	260.49	Redlands - Garden & Mariposa	23164357.AT2 23164-87.AT2 23164-UP.AT2
8527	547.45	Ground To Air Transmit And Receive Compound	CGATRHNN.AT2 CGATRHNE.AT2 CGATRHNZ.AT2

Table 1.10 Records used for Denali, Alaska, earthquake, 11/03/2002 (M7.9).

RSN	Hypocentral distance (km)	Station Name	File Name
2114	68.25	Carl	CARLO-90.AT2 CARLO360.AT2 CARLO-UP.AT2
2111	84.89	PS10	PS10-047.AT2 PS10-317.AT2 PS10-UP.AT2
2107	62.59	R109	R109-90.AT2 R109360.AT2 R109-UP.AT2
2112	115.82	PS08	PS08-49.AT2 PS08319.AT2 PS08-UP.AT2
3832	201.09	PS07	PS07-39.AT2 PS07309.AT2 PS07-UP.AT2
2104	296.96	8039	FS_7-90.AT2 FS_7360.AT2 FS_7-UP.AT2

1.13 OUTPUT FILE

This section describes the format of the output files. Fourier amplitude spectra are provided for the five time windows and will be used to populate the FAS flatfile. Figures 1.16 and 1.17 show examples of the FAS output file format for the entire window and the coda window, respectively. Note that the filtered and non-filtered FAS in Figure 1.16 are the same in the output file for the entire time history since the filtered recording in NGA-West2 are used without the application of any additional filter. The output file for the other four time windows (Figure 1.17) only populates the non-filtered FAS column, because the filters were chosen based on the FAS spectrum of the entire time series and not on these shorter time windows.

```
PEER NGA STRONG MOTION DATABASE FOURIER SPECTRA
Denali 11/03/2002, 8039, UP
ACCELERATION TIME HISTORY IN UNITS OF G
NPTS=  37560, DT=   0.005 SEC
***********************************************
FOURIER SPECTRA IN UNITS OF G-SEC
NPTS=   37560, DT=    0.005 SEC
           FREQ   NON-FILTERED       FILTERED
  0.0000000E+00  1.5852570E-06  1.5852570E-06
  7.6293945E-04  2.8228555E-06  2.8228555E-06
  1.5258789E-03  4.3865523E-06  4.3865523E-06
```

Figure 1.16 FAS example output file for an entire recording (Denali, Alaska, earthquake at station 8039, UP).

```
PEER NGA STRONG MOTION DATABASE FOURIER SPECTRA
Denali 11/03/2002, 8039, UP
ACCELERATION TIME HISTORY IN UNITS OF G
NPTS=  37560, DT=   0.005 SEC
*****************************************************
FOURIER SPECTRA IN UNITS OF G-SEC
NPTS=   12687, DT=    0.005 SEC, CODA-WINDOW UTILIZED
           FREQ   NON-FILTERED       FILTERED
  0.0000000E+00  4.7043412E-04
  7.6293945E-04  4.7056647E-04
  1.5258789E-03  4.7088923E-04
```

Figure 1.17 FAS example output file for a coda window (Denali, Alaska, earthquake at station 8039, UP).

1.14 SUMMARY

This report introduces a semi-automated approach for calculating FAS for the NGA-West2 acceleration time-history database. We devise and document a method for selecting time windows, and evaluate the method with the FAS computed from a suite of sample records with a range of different magnitudes and hypocentral distances that span the NGA-West2 dataset. A common frequency step (df) is used that allows more than 90% of the FAS to be used without interpolation to a common frequency. A zoom option facilitates accurate selection of *P*-arrival onset is a newly added feature to the standard PEER data processing code. Flags for late *P*-triggering, short-noise time window, short-coda time window, coda onset, and contamination of a window (i.e., one that includes an aftershock) have also been added as output metadata of this procedure and are to be included in the flatfile. These updates and flags to the data-processing code ensure the quality of the FAS database and allow the user to select FAS data in the NGA-West2 based on these criteria. Lastly, this report documents the output file format. This document will be updated if the data processing method is significantly revised. A FAS flatfile will be provided for the NGA-West2 database, based on implementation of the results and recommendations of this study.

REFERENCES

Abrahamson N.A. Silva W.J. (1997). Empirical response spectral attenuation relations for shallow crustal earthquakes, *Seismol. Res. Lett*., 68(1): 94–127.

Aki K. (1967). Scaling law of seismic spectrum, *J. Geophys. Res.,* 72: 1217–1231.

Aki K. (1969). Analysis of the seismic coda of local earthquakes as scattered waves, *J. Geophys. Res*., 74: 615–631.

Ancheta T.D., Darragh R.B., Stewart J.P., Seyhan E., Silva W.J., Chiou B.-S.J., Wooddell K.E., Graves R.W., Kottke A.R., Boore D.M., Kishida T., Donahue J.L. (2013). PEER NGA-West2 database, *PEER Report No. 2013/03*, Pacific Earthquake Engineering Research Center, University of California, Berkeley, CA.

Anderson J.G., Hough S.E. (1984). A model for the shape of the Fourier amplitude spectrum of acceleration at high frequencies, *Bull. Seismol. Soc. Am*., 74(5): 1969–1993.

Aoi S., Kunugi T., Fujiwara H. (2004). Strong-motion seismograph network operated by NIED: K-NET and KiK-net, *J. Japan Assoc. Earthq. Eng*., 4: 65–74.

Atkinson G.M., Silva W.J. (1997). An empirical study of earthquake source spectra for California earthquakes, *Bull. Seismol. Soc. Am*., 87: 97–113.

Brune J.N. (1970). Tectonic stress and the spectra of seismic shear waves from earthquakes, *J, Geophys, Res*., 75: 4997–5002.

Brune J.N. (1971). Correction, *J. Geophys. Res*., 76, pg. 5002.

Chiou B-S.J., Darragh R.B., Gregor N., Silva W.J. (2008). NGA project strong-motion database, *Earthq. Spectra*, 24(1): 23–44.

Goulet C.A., Kishida T., Ancheta T.D., Cramer C.H., Darragh R.B., Silva W.J., Hashash Y.M.A., Harmon J., Stewart J.P., Wooddell K.E., Youngs R.R. (2014). PEER NGA-East database, *PEER Report No. 2014/17*, Pacific Earthquake Engineering Research Center, University of California, Berkeley, CA.

Kato K., Aki K., Takemura M. (1995). Site amplification from coda waves: validation and application to S-wave site response, *Bull. Seismol. Soc. Am*., 85: 467–477.

Kempton J.J., Stewart J.P. (2006). Prediction equations for significant duration of earthquake ground motions considering site and near-source effects, *Earthq. Spectra*, 22: 985–1013.

Ktenidou O.-J., Abrahamson N.A, Darragh R.B., Silva W.J. (2016). A methodology for the estimation of kappa (κ) from large datasets, example application to rock sites in the NGA-East database, and implications on design motions, (in preparation), *PEER Report No. 2016/01*, Pacific Earthquake Engineering Research Center, University of California, Berkeley, CA.

Ktenidou O.-J., Cotton F., Abrahamson N.A., Anderson J.G. (2014). Taxonomy of kappa: a review of definitions and estimation methods targeted to applications, *Seismol. Res. Lett*., 85(1): 135–146.

Ktenidou O.-J., Gelis C., Bonilla F. (2013). A study on the variability of kappa in a borehole: Implications on the computation method used, *Bull. Seismol. Soc. Am.,* 103: 1048–1068.

Novelo-Casanova D.A., Lee W.H.K. (1991). Comparison of techniques that use the single scattering model to compute the quality factor Q from coda waves, *Pure Appl. Geophys*., 135: 77–89.

Ozacar A.A., Beck S.L. (2003). Source process of the 3 November 2002 Denali fault earthquake (central Alaska) from teleseismic observations, *Geophys. Res. Lett*., doi:10.1029/2003GL017272.

Padhy S., Subhadra N., Kayal J.R. (2011). Frequency-dependent attenuation of body and Coda waves in the Andaman Sea Basin, *Bull. Seismol. Soc. Am.,* 101: 109–125.

PEER (2015). NGA-East: Median ground-motion models for the Central and Eastern North America Region, Chapter 11, *PEER Report No. 2015/04*, Pacific Earthquake Engineering Research Center, University of California, Berkeley, CA.

Phillips S.W., Aki K. (1986). Site amplification of coda waves from local earthquakes in central California, *Bull. Seismol. Soc. Am*., 76: 627–648.

Satoh T., Kawase H., Matsushima S. (2001). Differences between site characteristics obtained from microtremors S-waves, P-waves, and codas. *Bull. Seismol. Soc. Am*., 91: 313–334.

Silva W.J. (2013). Personal Communication.

Wong V., Rebollar C.J., Munguia L. (2001). Attenuation of coda waves at Tres Vírgenes volcanic area, Baja California Sur, México, *Bull. Seismol. Soc. Am*., 91: 683–693.

PEER REPORTS

PEER reports are available as a free PDF download from http://peer.berkeley.edu/publications/peer_reports_complete.html. Printed hard copies of PEER reports can be ordered directly from our printer by following the instructions at http://peer.berkeley.edu/publications/peer_reports.html. For other related questions about the PEER Report Series, contact the Pacific Earthquake Engineering Research Center, 325 Davis Hall, Mail Code 1792, Berkeley, CA 94720. Tel.: (510) 642-3437; Fax: (510) 642-1655; Email: peer_editor@berkeley.edu.

PEER 2016/02 *Semi-Automated Procedure for Windowing time Series and Computing Fourier Amplitude Spectra for the NGA-West2 Database*. Tadahiro Kishida, Olga-Joan Ktenidou, Robert B. Darragh, and Walter J. Silva. May 2016.

PEER 2016/01 *A Methodology for the Estimation of Kappa (κ) from Large Datasets: Example Application to Rock Sites in the NGA-East Database and Implications on Design Motions.* Olga-Joan Ktenidou, Norman A. Abrahamson, Robert B. Darragh, and Walter J. Silva. April 2016.

PEER 2015/13 *Self-Centering Precast Concrete Dual-Steel-Shell Columns for Accelerated Bridge Construction: Seismic Performance, Analysis, and Design*. Gabriele Guerrini, José I. Restrepo, Athanassios Vervelidis, and Milena Massari. December 2015.

PEER 2015/12 *Shear-Flexure Interaction Modeling for Reinforced Concrete Structural Walls and Columns under Reversed Cyclic Loading*. Kristijan Kolozvari, Kutay Orakcal, and John Wallace. December 2015.

PEER 2015/11 *Selection and Scaling of Ground Motions for Nonlinear Response History Analysis of Buildings in Performance-Based Earthquake Engineering*. N. Simon Kwong and Anil K. Chopra. December 2015.

PEER 2015/10 *Structural Behavior of Column-Bent Cap Beam-Box Girder Systems in Reinforced Concrete Bridges Subjected to Gravity and Seismic Loads. Part II: Hybrid Simulation and Post-Test Analysis*. Mohamed A. Moustafa and Khalid M. Mosalam. November 2015.

PEER 2015/09 *Structural Behavior of Column-Bent Cap Beam-Box Girder Systems in Reinforced Concrete Bridges Subjected to Gravity and Seismic Loads. Part I: Pre-Test Analysis and Quasi-Static Experiments*. Mohamed A. Moustafa and Khalid M. Mosalam. September 2015.

PEER 2015/08 *NGA-East: Adjustments to Median Ground-Motion Models for Center and Eastern North America*. August 2015.

PEER 2015/07 *NGA-East: Ground-Motion Standard-Deviation Models for Central and Eastern North America*. Linda Al Atik. June 2015.

PEER 2015/06 *Adjusting Ground-Motion Intensity Measures to a Reference Site for which V_{S30} = 3000 m/sec*. David M. Boore. May 2015.

PEER 2015/05 *Hybrid Simulation of Seismic Isolation Systems Applied to an APR-1400 Nuclear Power Plant.* Andreas H. Schellenberg, Alireza Sarebanha, Matthew J. Schoettler, Gilberto Mosqueda, Gianmario Benzoni, and Stephen A. Mahin. April 2015.

PEER 2015/04 *NGA-East: Median Ground-Motion Models for the Central and Eastern North America Region*. April 2015.

PEER 2015/03 *Single Series Solution for the Rectangular Fiber-Reinforced Elastomeric Isolator Compression Modulus*. James M. Kelly and Niel C. Van Engelen. March 2015.

PEER 2015/02 *A Full-Scale, Single-Column Bridge Bent Tested by Shake-Table Excitation.* Matthew J. Schoettler, José I. Restrepo, Gabriele Guerrini, David E. Duck, and Francesco Carrea. March 2015.

PEER 2015/01 *Concrete Column Blind Prediction Contest 2010: Outcomes and Observations.* Vesna Terzic, Matthew J. Schoettler, José I. Restrepo, and Stephen A Mahin. March 2015.

PEER 2014/20 *Stochastic Modeling and Simulation of Near-Fault Ground Motions for Performance-Based Earthquake Engineering*. Mayssa Dabaghi and Armen Der Kiureghian. December 2014.

PEER 2014/19 *Seismic Response of a Hybrid Fiber-Reinforced Concrete Bridge Column Detailed for Accelerated Bridge Construction*. Wilson Nguyen, William Trono, Marios Panagiotou, and Claudia P. Ostertag. December 2014.

PEER 2014/18 *Three-Dimensional Beam-Truss Model for Reinforced Concrete Walls and Slabs Subjected to Cyclic Static or Dynamic Loading*. Yuan Lu, Marios Panagiotou, and Ioannis Koutromanos. December 2014.

PEER 2014/17 *PEER NGA-East Database.* Christine A. Goulet, Tadahiro Kishida, Timothy D. Ancheta, Chris H. Cramer, Robert B. Darragh, Walter J. Silva, Youssef M.A. Hashash, Joseph Harmon, Jonathan P. Stewart, Katie E. Wooddell, and Robert R. Youngs. October 2014.

PEER 2014/16 *Guidelines for Performing Hazard-Consistent One-Dimensional Ground Response Analysis for Ground Motion Prediction*. Jonathan P. Stewart, Kioumars Afshari, and Youssef M.A. Hashash. October 2014.

PEER 2014/15 *NGA-East Regionalization Report: Comparison of Four Crustal Regions within Central and Eastern North America using Waveform Modeling and 5%-Damped Pseudo-Spectral Acceleration Response*. Jennifer Dreiling, Marius P. Isken, Walter D. Mooney, Martin C. Chapman, and Richard W. Godbee. October 2014.

PEER 2014/14 *Scaling Relations between Seismic Moment and Rupture Area of Earthquakes in Stable Continental Regions*. Paul Somerville. August 2014.

PEER 2014/13 *PEER Preliminary Notes and Observations on the August 24, 2014, South Napa Earthquake*. Grace S. Kang and Stephen A. Mahin, Editors. September 2014.

PEER 2014/12 *Reference-Rock Site Conditions for Central and Eastern North America: Part II – Attenuation (Kappa) Definition*. Kenneth W. Campbell, Youssef M.A. Hashash, Byungmin Kim, Albert R. Kottke, Ellen M. Rathje, Walter J. Silva, and Jonathan P. Stewart. August 2014.

PEER 2014/11 *Reference-Rock Site Conditions for Central and Eastern North America: Part I - Velocity Definition*. Youssef M.A. Hashash, Albert R. Kottke, Jonathan P. Stewart, Kenneth W. Campbell, Byungmin Kim, Ellen M. Rathje, Walter J. Silva, Sissy Nikolaou, and Cheryl Moss. August 2014.

PEER 2014/10 *Evaluation of Collapse and Non-Collapse of Parallel Bridges Affected by Liquefaction and Lateral Spreading*. Benjamin Turner, Scott J. Brandenberg, and Jonathan P. Stewart. August 2014.

PEER 2014/09 *PEER Arizona Strong-Motion Database and GMPEs Evaluation*. Tadahiro Kishida, Robert E. Kayen, Olga-Joan Ktenidou, Walter J. Silva, Robert B. Darragh, and Jennie Watson-Lamprey. June 2014.

PEER 2014/08 *Unbonded Pretensioned Bridge Columns with Rocking Detail*. Jeffrey A. Schaefer, Bryan Kennedy, Marc O. Eberhard, and John F. Stanton. June 2014.

PEER 2014/07 *Northridge 20 Symposium Summary Report: Impacts, Outcomes, and Next Steps*. May 2014.

PEER 2014/06 *Report of the Tenth Planning Meeting of NEES/E-Defense Collaborative Research on Earthquake Engineering*. December 2013.

PEER 2014/05 *Seismic Velocity Site Characterization of Thirty-One Chilean Seismometer Stations by Spectral Analysis of Surface Wave Dispersion*. Robert Kayen, Brad D. Carkin, Skye Corbet, Camilo Pinilla, Allan Ng, Edward Gorbis, and Christine Truong. April 2014.

PEER 2014/04 Effect of Vertical Acceleration on Shear Strength of Reinforced Concrete Columns. Hyerin Lee and Khalid M. Mosalam. April 2014.

PEER 2014/03 *Retest of Thirty-Year-Old Neoprene Isolation Bearings.* James M. Kelly and Niel C. Van Engelen. March 2014.

PEER 2014/02 *Theoretical Development of Hybrid Simulation Applied to Plate Structures.* Ahmed A. Bakhaty, Khalid M. Mosalam, and Sanjay Govindjee. January 2014.

PEER 2014/01 *Performance-Based Seismic Assessment of Skewed Bridges.* Peyman Kaviani, Farzin Zareian, and Ertugrul Taciroglu. January 2014.

PEER 2013/26 *Urban Earthquake Engineerin*g. Proceedings of the U.S.-Iran Seismic Workshop. December 2013.

PEER 2013/25 *Earthquake Engineering for Resilient Communities: 2013 PEER Internship Program Research Report Collection.* Heidi Tremayne (Editor), Stephen A. Mahin (Editor), Jorge Archbold Monterossa, Matt Brosman, Shelly Dean, Katherine deLaveaga, Curtis Fong, Donovan Holder, Rakeeb Khan, Elizabeth Jachens, David Lam, Daniela Martinez Lopez, Mara Minner, Geffen Oren, Julia Pavicic, Melissa Quinonez, Lorena Rodriguez, Sean Salazar, Kelli Slaven, Vivian Steyert, Jenny Taing, and Salvador Tena. December 2013.

PEER 2013/24 *NGA-West2 Ground Motion Prediction Equations for Vertical Ground Motions*. September 2013.

PEER 2013/23 *Coordinated Planning and Preparedness for Fire Following Major Earthquakes*. Charles Scawthorn. November 2013.

PEER 2013/22 *GEM-PEER Task 3 Project: Selection of a Global Set of Ground Motion Prediction Equations.* Jonathan P. Stewart, John Douglas, Mohammad B. Javanbarg, Carola Di Alessandro, Yousef Bozorgnia, Norman A. Abrahamson, David M. Boore, Kenneth W. Campbell, Elise Delavaud, Mustafa Erdik, and Peter J. Stafford. December 2013.

PEER 2013/21 *Seismic Design and Performance of Bridges with Columns on Rocking Foundations*. Grigorios Antonellis and Marios Panagiotou. September 2013.

PEER 2013/20 *Experimental and Analytical Studies on the Seismic Behavior of Conventional and Hybrid Braced Frames*. Jiun-Wei Lai and Stephen A. Mahin. September 2013.

PEER 2013/19 *Toward Resilient Communities: A Performance-Based Engineering Framework for Design and Evaluation of the Built Environment.* Michael William Mieler, Bozidar Stojadinovic, Robert J. Budnitz, Stephen A. Mahin, and Mary C. Comerio. September 2013.

PEER 2013/18 *Identification of Site Parameters that Improve Predictions of Site Amplification*. Ellen M. Rathje and Sara Navidi. July 2013.

PEER 2013/17 *Response Spectrum Analysis of Concrete Gravity Dams Including Dam-Water-Foundation Interaction*. Arnkjell Løkke and Anil K. Chopra. July 2013.

PEER 2013/16 *Effect of Hoop Reinforcement Spacing on the Cyclic Response of Large Reinforced Concrete Special Moment Frame Beams.* Marios Panagiotou, Tea Visnjic, Grigorios Antonellis, Panagiotis Galanis, and Jack P. Moehle. June 2013.

PEER 2013/15 *A Probabilistic Framework to Include the Effects of Near-Fault Directivity in Seismic Hazard Assessment*. Shrey Kumar Shahi, Jack W. Baker. October 2013.

PEER 2013/14 *Hanging-Wall Scaling using Finite-Fault Simulations.* Jennifer L. Donahue and Norman A. Abrahamson. September 2013.

PEER 2013/13 *Semi-Empirical Nonlinear Site Amplification and its Application in NEHRP Site Factors*. Jonathan P. Stewart and Emel Seyhan. November 2013.

PEER 2013/12 *Nonlinear Horizontal Site Response for the NGA-West2 Project.* Ronnie Kamai, Norman A. Abramson, Walter J. Silva. May 2013.

PEER 2013/11 *Epistemic Uncertainty for NGA-West2 Models.* Linda Al Atik and Robert R. Youngs. May 2013.

PEER 2013/10 *NGA-West 2 Models for Ground-Motion Directionality.* Shrey K. Shahi and Jack W. Baker. May 2013.

PEER 2013/09 *Final Report of the NGA-West2 Directivity Working Group.* Paul Spudich, Jeffrey R. Bayless, Jack W. Baker, Brian S.J. Chiou, Badie Rowshandel, Shrey Shahi, and Paul Somerville. May 2013.

PEER 2013/08 *NGA-West2 Model for Estimating Average Horizontal Values of Pseudo-Absolute Spectral Accelerations Generated by Crustal Earthquakes*. I. M. Idriss. May 2013.

PEER 2013/07 *Update of the Chiou and Youngs NGA Ground Motion Model for Average Horizontal Component of Peak Ground Motion and Response Spectra*. Brian Chiou and Robert Youngs. May 2013.

PEER 2013/06 *NGA-West2 Campbell-Bozorgnia Ground Motion Model for the Horizontal Components of PGA, PGV, and 5%-Damped Elastic Pseudo-Acceleration Response Spectra for Periods Ranging from 0.01 to 10 sec.* Kenneth W. Campbell and Yousef Bozorgnia. May 2013.

PEER 2013/05 *NGA-West 2 Equations for Predicting Response Spectral Accelerations for Shallow Crustal Earthquakes*. David M. Boore, Jonathan P. Stewart, Emel Seyhan, and Gail M. Atkinson. May 2013.

PEER 2013/04 *Update of the AS08 Ground-Motion Prediction Equations Based on the NGA-West2 Data Set*. Norman Abrahamson, Walter Silva, and Ronnie Kamai. May 2013.

PEER 2013/03 *PEER NGA-West2 Database.* Timothy D. Ancheta, Robert B. Darragh, Jonathan P. Stewart, Emel Seyhan, Walter J. Silva, Brian S.J. Chiou, Katie E. Wooddell, Robert W. Graves, Albert R. Kottke, David M. Boore, Tadahiro Kishida, and Jennifer L. Donahue. May 2013.

PEER 2013/02 *Hybrid Simulation of the Seismic Response of Squat Reinforced Concrete Shear Walls*. Catherine A. Whyte and Bozidar Stojadinovic. May 2013.

PEER 2013/01 *Housing Recovery in Chile: A Qualitative Mid-program Review*. Mary C. Comerio. February 2013.

PEER 2012/08 *Guidelines for Estimation of Shear Wave Velocity.* Bernard R. Wair, Jason T. DeJong, and Thomas Shantz. December 2012.

PEER 2012/07 *Earthquake Engineering for Resilient Communities: 2012 PEER Internship Program Research Report Collection.* Heidi Tremayne (Editor), Stephen A. Mahin (Editor), Collin Anderson, Dustin Cook, Michael Erceg, Carlos Esparza, Jose Jimenez, Dorian Krausz, Andrew Lo, Stephanie Lopez, Nicole McCurdy, Paul Shipman, Alexander Strum, Eduardo Vega. December 2012.

PEER 2012/06 *Fragilities for Precarious Rocks at Yucca Mountain.* Matthew D. Purvance, Rasool Anooshehpoor, and James N. Brune. December 2012.

PEER 2012/05 *Development of Simplified Analysis Procedure for Piles in Laterally Spreading Layered Soils.* Christopher R. McGann, Pedro Arduino, and Peter Mackenzie–Helnwein. December 2012.

PEER 2012/04 *Unbonded Pre-Tensioned Columns for Bridges in Seismic Regions.* Phillip M. Davis, Todd M. Janes, Marc O. Eberhard, and John F. Stanton. December 2012.

PEER 2012/03 *Experimental and Analytical Studies on Reinforced Concrete Buildings with Seismically Vulnerable Beam-Column Joints*. Sangjoon Park and Khalid M. Mosalam. October 2012.

PEER 2012/02 *Seismic Performance of Reinforced Concrete Bridges Allowed to Uplift during Multi-Directional Excitation*. Andres Oscar Espinoza and Stephen A. Mahin. July 2012.

PEER 2012/01 *Spectral Damping Scaling Factors for Shallow Crustal Earthquakes in Active Tectonic Regions.* Sanaz Rezaeian, Yousef Bozorgnia, I. M. Idriss, Kenneth Campbell, Norman Abrahamson, and Walter Silva. July 2012.

PEER 2011/10 *Earthquake Engineering for Resilient Communities: 2011 PEER Internship Program Research Report Collection*. Heidi Faison and Stephen A. Mahin, Editors. December 2011.

PEER 2011/09 *Calibration of Semi-Stochastic Procedure for Simulating High-Frequency Ground Motions*. Jonathan P. Stewart, Emel Seyhan, and Robert W. Graves. December 2011.

PEER 2011/08 *Water Supply in regard to Fire Following Earthquake*. Charles Scawthorn. November 2011.

PEER 2011/07 *Seismic Risk Management in Urban Areas*. Proceedings of a U.S.-Iran-Turkey Seismic Workshop. September 2011.

PEER 2011/06 *The Use of Base Isolation Systems to Achieve Complex Seismic Performance Objectives*. Troy A. Morgan and Stephen A. Mahin. July 2011.

PEER 2011/05 *Case Studies of the Seismic Performance of Tall Buildings Designed by Alternative Means.* Task 12 Report for the Tall Buildings Initiative. Jack Moehle, Yousef Bozorgnia, Nirmal Jayaram, Pierson Jones, Mohsen Rahnama, Nilesh Shome, Zeynep Tuna, John Wallace, Tony Yang, and Farzin Zareian. July 2011.

PEER 2011/04 *Recommended Design Practice for Pile Foundations in Laterally Spreading Ground.* Scott A. Ashford, Ross W. Boulanger, and Scott J. Brandenberg. June 2011.

PEER 2011/03 *New Ground Motion Selection Procedures and Selected Motions for the PEER Transportation Research Program*. Jack W. Baker, Ting Lin, Shrey K. Shahi, and Nirmal Jayaram. March 2011.

PEER 2011/02 *A Bayesian Network Methodology for Infrastructure Seismic Risk Assessment and Decision Support*. Michelle T. Bensi, Armen Der Kiureghian, and Daniel Straub. March 2011.

PEER 2011/01 *Demand Fragility Surfaces for Bridges in Liquefied and Laterally Spreading Ground.* Scott J. Brandenberg, Jian Zhang, Pirooz Kashighandi, Yili Huo, and Minxing Zhao. March 2011.

PEER 2010/05 *Guidelines for Performance-Based Seismic Design of Tall Buildings.* Developed by the Tall Buildings Initiative. November 2010.

PEER 2010/04 *Application Guide for the Design of Flexible and Rigid Bus Connections between Substation Equipment Subjected to Earthquakes.* Jean-Bernard Dastous and Armen Der Kiureghian. September 2010.

PEER 2010/03 *Shear Wave Velocity as a Statistical Function of Standard Penetration Test Resistance and Vertical Effective Stress at Caltrans Bridge Sites.* Scott J. Brandenberg, Naresh Bellana, and Thomas Shantz. June 2010.

PEER 2010/02 *Stochastic Modeling and Simulation of Ground Motions for Performance-Based Earthquake Engineering.* Sanaz Rezaeian and Armen Der Kiureghian. June 2010.

PEER 2010/01 *Structural Response and Cost Characterization of Bridge Construction Using Seismic Performance Enhancement Strategies.* Ady Aviram, Božidar Stojadinović, Gustavo J. Parra-Montesinos, and Kevin R. Mackie. March 2010.

PEER 2009/03 *The Integration of Experimental and Simulation Data in the Study of Reinforced Concrete Bridge Systems Including Soil-Foundation-Structure Interaction.* Matthew Dryden and Gregory L. Fenves. November 2009.

PEER 2009/02 *Improving Earthquake Mitigation through Innovations and Applications in Seismic Science, Engineering, Communication, and Response*. Proceedings of a U.S.-Iran Seismic Workshop. October 2009.

PEER 2009/01 *Evaluation of Ground Motion Selection and Modification Methods: Predicting Median Interstory Drift Response of Buildings*. Curt B. Haselton, Editor. June 2009.

PEER 2008/10 *Technical Manual for Strata.* Albert R. Kottke and Ellen M. Rathje. February 2009.

PEER 2008/09 *NGA Model for Average Horizontal Component of Peak Ground Motion and Response Spectra.* Brian S.-J. Chiou and Robert R. Youngs. November 2008.

PEER 2008/08 *Toward Earthquake-Resistant Design of Concentrically Braced Steel Structures*. Patxi Uriz and Stephen A. Mahin. November 2008.

PEER 2008/07 *Using OpenSees for Performance-Based Evaluation of Bridges on Liquefiable Soils*. Stephen L. Kramer, Pedro Arduino, and HyungSuk Shin. November 2008.

PEER 2008/06 *Shaking Table Tests and Numerical Investigation of Self-Centering Reinforced Concrete Bridge Columns*. Hyung IL Jeong, Junichi Sakai, and Stephen A. Mahin. September 2008.

PEER 2008/05 *Performance-Based Earthquake Engineering Design Evaluation Procedure for Bridge Foundations Undergoing Liquefaction-Induced Lateral Ground Displacement*. Christian A. Ledezma and Jonathan D. Bray. August 2008.

PEER 2008/04 *Benchmarking of Nonlinear Geotechnical Ground Response Analysis Procedures.* Jonathan P. Stewart, Annie On-Lei Kwok, Yousseff M. A. Hashash, Neven Matasovic, Robert Pyke, Zhiliang Wang, and Zhaohui Yang. August 2008.

PEER 2008/03 *Guidelines for Nonlinear Analysis of Bridge Structures in California.* Ady Aviram, Kevin R. Mackie, and Božidar Stojadinović. August 2008.

PEER 2008/02 *Treatment of Uncertainties in Seismic-Risk Analysis of Transportation Systems*. Evangelos Stergiou and Anne S. Kiremidjian. July 2008.

PEER 2008/01 *Seismic Performance Objectives for Tall Buildings.* William T. Holmes, Charles Kircher, William Petak, and Nabih Youssef. August 2008.

PEER 2007/12 *An Assessment to Benchmark the Seismic Performance of a Code-Conforming Reinforced Concrete Moment-Frame Building.* Curt Haselton, Christine A. Goulet, Judith Mitrani-Reiser, James L. Beck, Gregory G. Deierlein, Keith A. Porter, Jonathan P. Stewart, and Ertugrul Taciroglu. August 2008.

PEER 2007/11 *Bar Buckling in Reinforced Concrete Bridge Columns.* Wayne A. Brown, Dawn E. Lehman, and John F. Stanton. February 2008.

PEER 2007/10 *Computational Modeling of Progressive Collapse in Reinforced Concrete Frame Structures*. Mohamed M. Talaat and Khalid M. Mosalam. May 2008.

PEER 2007/09 *Integrated Probabilistic Performance-Based Evaluation of Benchmark Reinforced Concrete Bridges*. Kevin R. Mackie, John-Michael Wong, and Božidar Stojadinović. January 2008.

PEER 2007/08 *Assessing Seismic Collapse Safety of Modern Reinforced Concrete Moment-Frame Buildings*. Curt B. Haselton and Gregory G. Deierlein. February 2008.

PEER 2007/07 *Performance Modeling Strategies for Modern Reinforced Concrete Bridge Columns*. Michael P. Berry and Marc O. Eberhard. April 2008.

PEER 2007/06 *Development of Improved Procedures for Seismic Design of Buried and Partially Buried Structures*. Linda Al Atik and Nicholas Sitar. June 2007.

PEER 2007/05 *Uncertainty and Correlation in Seismic Risk Assessment of Transportation Systems*. Renee G. Lee and Anne S. Kiremidjian. July 2007.

PEER 2007/04 *Numerical Models for Analysis and Performance-Based Design of Shallow Foundations Subjected to Seismic Loading.* Sivapalan Gajan, Tara C. Hutchinson, Bruce L. Kutter, Prishati Raychowdhury, José A. Ugalde, and Jonathan P. Stewart. May 2008.

PEER 2007/03 *Beam-Column Element Model Calibrated for Predicting Flexural Response Leading to Global Collapse of RC Frame Buildings*. Curt B. Haselton, Abbie B. Liel, Sarah Taylor Lange, and Gregory G. Deierlein. May 2008.

PEER 2007/02 *Campbell-Bozorgnia NGA Ground Motion Relations for the Geometric Mean Horizontal Component of Peak and Spectral Ground Motion Parameters*. Kenneth W. Campbell and Yousef Bozorgnia. May 2007.

PEER 2007/01 *Boore-Atkinson NGA Ground Motion Relations for the Geometric Mean Horizontal Component of Peak and Spectral Ground Motion Parameters*. David M. Boore and Gail M. Atkinson. May 2007.

PEER 2006/12 Societal Implications of Performance-Based Earthquake Engineering. Peter J. May. May 2007.

PEER 2006/11 *Probabilistic Seismic Demand Analysis Using Advanced Ground Motion Intensity Measures, Attenuation Relationships, and Near-Fault Effects*. Polsak Tothong and C. Allin Cornell. March 2007.

PEER 2006/10 *Application of the PEER PBEE Methodology to the I-880 Viaduct*. Sashi Kunnath. February 2007.

PEER 2006/09 *Quantifying Economic Losses from Travel Forgone Following a Large Metropolitan Earthquake*. James Moore, Sungbin Cho, Yue Yue Fan, and Stuart Werner. November 2006.

PEER 2006/08 *Vector-Valued Ground Motion Intensity Measures for Probabilistic Seismic Demand Analysis*. Jack W. Baker and C. Allin Cornell. October 2006.

PEER 2006/07 *Analytical Modeling of Reinforced Concrete Walls for Predicting Flexural and Coupled–Shear-Flexural Responses*. Kutay Orakcal, Leonardo M. Massone, and John W. Wallace. October 2006.

PEER 2006/06 *Nonlinear Analysis of a Soil-Drilled Pier System under Static and Dynamic Axial Loading*. Gang Wang and Nicholas Sitar. November 2006.

PEER 2006/05 *Advanced Seismic Assessment Guidelines.* Paolo Bazzurro, C. Allin Cornell, Charles Menun, Maziar Motahari, and Nicolas Luco. September 2006.

PEER 2006/04 *Probabilistic Seismic Evaluation of Reinforced Concrete Structural Components and Systems*. Tae Hyung Lee and Khalid M. Mosalam. August 2006.

PEER 2006/03 *Performance of Lifelines Subjected to Lateral Spreading.* Scott A. Ashford and Teerawut Juirnarongrit. July 2006.

PEER 2006/02 *Pacific Earthquake Engineering Research Center Highway Demonstration Project.* Anne Kiremidjian, James Moore, Yue Yue Fan, Nesrin Basoz, Ozgur Yazali, and Meredith Williams. April 2006.

PEER 2006/01 *Bracing Berkeley. A Guide to Seismic Safety on the UC Berkeley Campus.* Mary C. Comerio, Stephen Tobriner, and Ariane Fehrenkamp. January 2006.

PEER 2005/16 *Seismic Response and Reliability of Electrical Substation Equipment and Systems.* Junho Song, Armen Der Kiureghian, and Jerome L. Sackman. April 2006.

PEER 2005/15 *CPT-Based Probabilistic Assessment of Seismic Soil Liquefaction Initiation.* R. E. S. Moss, R. B. Seed, R. E. Kayen, J. P. Stewart, and A. Der Kiureghian. April 2006.

PEER 2005/14 *Workshop on Modeling of Nonlinear Cyclic Load-Deformation Behavior of Shallow Foundations.* Bruce L. Kutter, Geoffrey Martin, Tara Hutchinson, Chad Harden, Sivapalan Gajan, and Justin Phalen. March 2006.

PEER 2005/13 *Stochastic Characterization and Decision Bases under Time-Dependent Aftershock Risk in Performance-Based Earthquake Engineering*. Gee Liek Yeo and C. Allin Cornell. July 2005.

PEER 2005/12 *PEER Testbed Study on a Laboratory Building: Exercising Seismic Performance Assessment.* Mary C. Comerio, Editor. November 2005.

PEER 2005/11 *Van Nuys Hotel Building Testbed Report: Exercising Seismic Performance Assessment.* Helmut Krawinkler, Editor. October 2005.

PEER 2005/10 *First NEES/E-Defense Workshop on Collapse Simulation of Reinforced Concrete Building Structures.* September 2005.

PEER 2005/09 *Test Applications of Advanced Seismic Assessment Guidelines.* Joe Maffei, Karl Telleen, Danya Mohr, William Holmes, and Yuki Nakayama. August 2006.

PEER 2005/08 *Damage Accumulation in Lightly Confined Reinforced Concrete Bridge Columns.* R. Tyler Ranf, Jared M. Nelson, Zach Price, Marc O. Eberhard, and John F. Stanton. April 2006.

PEER 2005/07 *Experimental and Analytical Studies on the Seismic Response of Freestanding and Anchored Laboratory Equipment.* Dimitrios Konstantinidis and Nicos Makris. January 2005.

PEER 2005/06 *Global Collapse of Frame Structures under Seismic Excitations*. Luis F. Ibarra and Helmut Krawinkler. September 2005.

PEER 2005//05 *Performance Characterization of Bench- and Shelf-Mounted Equipment.* Samit Ray Chaudhuri and Tara C. Hutchinson. May 2006.

PEER 2005/04 *Numerical Modeling of the Nonlinear Cyclic Response of Shallow Foundations.* Chad Harden, Tara Hutchinson, Geoffrey R. Martin, and Bruce L. Kutter. August 2005.

PEER 2005/03 *A Taxonomy of Building Components for Performance-Based Earthquake Engineering.* Keith A. Porter. September 2005.

PEER 2005/02 *Fragility Basis for California Highway Overpass Bridge Seismic Decision Making*. Kevin R. Mackie and Božidar Stojadinović. June 2005.

PEER 2005/01 *Empirical Characterization of Site Conditions on Strong Ground Motion.* Jonathan P. Stewart, Yoojoong Choi, and Robert W. Graves. June 2005.

PEER 2004/09 *Electrical Substation Equipment Interaction: Experimental Rigid Conductor Studies.* Christopher Stearns and André Filiatrault. February 2005.

PEER 2004/08 *Seismic Qualification and Fragility Testing of Line Break 550-kV Disconnect Switches.* Shakhzod M. Takhirov, Gregory L. Fenves, and Eric Fujisaki. January 2005.

PEER 2004/07 *Ground Motions for Earthquake Simulator Qualification of Electrical Substation Equipment.* Shakhzod M. Takhirov, Gregory L. Fenves, Eric Fujisaki, and Don Clyde. January 2005.

PEER 2004/06 *Performance-Based Regulation and Regulatory Regimes.* Peter J. May and Chris Koski. September 2004.

PEER 2004/05 *Performance-Based Seismic Design Concepts and Implementation: Proceedings of an International Workshop.* Peter Fajfar and Helmut Krawinkler, Editors. September 2004.

PEER 2004/04 *Seismic Performance of an Instrumented Tilt-up Wall Building.* James C. Anderson and Vitelmo V. Bertero. July 2004.

PEER 2004/03 *Evaluation and Application of Concrete Tilt-up Assessment Methodologies.* Timothy Graf and James O. Malley. October 2004.

PEER 2004/02 *Analytical Investigations of New Methods for Reducing Residual Displacements of Reinforced Concrete Bridge Columns.* Junichi Sakai and Stephen A. Mahin. August 2004.

PEER 2004/01 *Seismic Performance of Masonry Buildings and Design Implications.* Kerri Anne Taeko Tokoro, James C. Anderson, and Vitelmo V. Bertero. February 2004.

PEER 2003/18 *Performance Models for Flexural Damage in Reinforced Concrete Columns.* Michael Berry and Marc Eberhard. August 2003.

PEER 2003/17 *Predicting Earthquake Damage in Older Reinforced Concrete Beam-Column Joints.* Catherine Pagni and Laura Lowes. October 2004.

PEER 2003/16 *Seismic Demands for Performance-Based Design of Bridges.* Kevin Mackie and Božidar Stojadinović. August 2003.

PEER 2003/15 *Seismic Demands for Nondeteriorating Frame Structures and Their Dependence on Ground Motions.* Ricardo Antonio Medina and Helmut Krawinkler. May 2004.

PEER 2003/14 *Finite Element Reliability and Sensitivity Methods for Performance-Based Earthquake Engineering*. Terje Haukaas and Armen Der Kiureghian. April 2004.

PEER 2003/13 *Effects of Connection Hysteretic Degradation on the Seismic Behavior of Steel Moment-Resisting Frames.* Janise E. Rodgers and Stephen A. Mahin. March 2004.

PEER 2003/12 *Implementation Manual for the Seismic Protection of Laboratory Contents: Format and Case Studies*. William T. Holmes and Mary C. Comerio. October 2003.

PEER 2003/11 *Fifth U.S.-Japan Workshop on Performance-Based Earthquake Engineering Methodology for Reinforced Concrete Building Structures*. February 2004.

PEER 2003/10 *A Beam-Column Joint Model for Simulating the Earthquake Response of Reinforced Concrete Frames.* Laura N. Lowes, Nilanjan Mitra, and Arash Altoontash. February 2004.

PEER 2003/09 *Sequencing Repairs after an Earthquake: An Economic Approach.* Marco Casari and Simon J. Wilkie. April 2004.

PEER 2003/08 *A Technical Framework for Probability-Based Demand and Capacity Factor Design (DCFD) Seismic Formats*. Fatemeh Jalayer and C. Allin Cornell. November 2003.

PEER 2003/07 *Uncertainty Specification and Propagation for Loss Estimation Using FOSM Methods.* Jack W. Baker and C. Allin Cornell. September 2003.

PEER 2003/06 *Performance of Circular Reinforced Concrete Bridge Columns under Bidirectional Earthquake Loading*. Mahmoud M. Hachem, Stephen A. Mahin, and Jack P. Moehle. February 2003.

PEER 2003/05 *Response Assessment for Building-Specific Loss Estimation.* Eduardo Miranda and Shahram Taghavi. September 2003.

PEER 2003/04 *Experimental Assessment of Columns with Short Lap Splices Subjected to Cyclic Loads*. Murat Melek, John W. Wallace, and Joel Conte. April 2003.

PEER 2003/03 *Probabilistic Response Assessment for Building-Specific Loss Estimation*. Eduardo Miranda and Hesameddin Aslani. September 2003.

PEER 2003/02 *Software Framework for Collaborative Development of Nonlinear Dynamic Analysis Program*. Jun Peng and Kincho H. Law. September 2003.

PEER 2003/01 *Shake Table Tests and Analytical Studies on the Gravity Load Collapse of Reinforced Concrete Frames.* Kenneth John Elwood and Jack P. Moehle. November 2003.

PEER 2002/24 *Performance of Beam to Column Bridge Joints Subjected to a Large Velocity Pulse.* Natalie Gibson, André Filiatrault, and Scott A. Ashford. April 2002.

PEER 2002/23 *Effects of Large Velocity Pulses on Reinforced Concrete Bridge Columns.* Greg L. Orozco and Scott A. Ashford. April 2002.

PEER 2002/22 *Characterization of Large Velocity Pulses for Laboratory Testing.* Kenneth E. Cox and Scott A. Ashford. April 2002.

PEER 2002/21 *Fourth U.S.-Japan Workshop on Performance-Based Earthquake Engineering Methodology for Reinforced Concrete Building Structures*. December 2002.

PEER 2002/20 *Barriers to Adoption and Implementation of PBEE Innovations.* Peter J. May. August 2002.

PEER 2002/19 *Economic-Engineered Integrated Models for Earthquakes: Socioeconomic Impacts.* Peter Gordon, James E. Moore II, and Harry W. Richardson. July 2002.

PEER 2002/18 *Assessment of Reinforced Concrete Building Exterior Joints with Substandard Details.* Chris P. Pantelides, Jon Hansen, Justin Nadauld, and Lawrence D. Reaveley. May 2002.

PEER 2002/17 *Structural Characterization and Seismic Response Analysis of a Highway Overcrossing Equipped with Elastomeric Bearings and Fluid Dampers: A Case Study*. Nicos Makris and Jian Zhang. November 2002.

PEER 2002/16 *Estimation of Uncertainty in Geotechnical Properties for Performance-Based Earthquake Engineering*. Allen L. Jones, Steven L. Kramer, and Pedro Arduino. December 2002.

PEER 2002/15 *Seismic Behavior of Bridge Columns Subjected to Various Loading Patterns*. Asadollah Esmaeily-Gh. and Yan Xiao. December 2002.

PEER 2002/14 *Inelastic Seismic Response of Extended Pile Shaft Supported Bridge Structures.* T.C. Hutchinson, R.W. Boulanger, Y.H. Chai, and I.M. Idriss. December 2002.

PEER 2002/13 *Probabilistic Models and Fragility Estimates for Bridge Components and Systems.* Paolo Gardoni, Armen Der Kiureghian, and Khalid M. Mosalam. June 2002.

PEER 2002/12 *Effects of Fault Dip and Slip Rake on Near-Source Ground Motions: Why Chi-Chi Was a Relatively Mild M7.6 Earthquake*. Brad T. Aagaard, John F. Hall, and Thomas H. Heaton. December 2002.

PEER 2002/11 *Analytical and Experimental Study of Fiber-Reinforced Strip Isolators*. James M. Kelly and Shakhzod M. Takhirov. September 2002.

PEER 2002/10 *Centrifuge Modeling of Settlement and Lateral Spreading with Comparisons to Numerical Analyses***.** Sivapalan Gajan and Bruce L. Kutter. January 2003.

PEER 2002/09 *Documentation and Analysis of Field Case Histories of Seismic Compression during the 1994 Northridge, California, Earthquake*. Jonathan P. Stewart, Patrick M. Smith, Daniel H. Whang, and Jonathan D. Bray. October 2002.

PEER 2002/08 *Component Testing, Stability Analysis and Characterization of Buckling-Restrained Unbonded Braces^{TM}*. Cameron Black, Nicos Makris, and Ian Aiken. September 2002.

PEER 2002/07 *Seismic Performance of Pile-Wharf Connections.* Charles W. Roeder, Robert Graff, Jennifer Soderstrom, and Jun Han Yoo. December 2001.

PEER 2002/06 *The Use of Benefit-Cost Analysis for Evaluation of Performance-Based Earthquake Engineering Decisions.* Richard O. Zerbe and Anthony Falit-Baiamonte. September 2001.

PEER 2002/05 *Guidelines, Specifications, and Seismic Performance Characterization of Nonstructural Building Components and Equipment*. André Filiatrault, Constantin Christopoulos, and Christopher Stearns. September 2001.

PEER 2002/04 *Consortium of Organizations for Strong-Motion Observation Systems and the Pacific Earthquake Engineering Research Center Lifelines Program: Invited Workshop on Archiving and Web Dissemination of Geotechnical Data, 4–5 October 2001*. September 2002.

PEER 2002/03 *Investigation of Sensitivity of Building Loss Estimates to Major Uncertain Variables for the Van Nuys Testbed*. Keith A. Porter, James L. Beck, and Rustem V. Shaikhutdinov. August 2002.

PEER 2002/02 *The Third U.S.-Japan Workshop on Performance-Based Earthquake Engineering Methodology for Reinforced Concrete Building Structures*. July 2002.

PEER 2002/01 *Nonstructural Loss Estimation: The UC Berkeley Case Study.* Mary C. Comerio and John C. Stallmeyer. December 2001.

PEER 2001/16 *Statistics of SDF-System Estimate of Roof Displacement for Pushover Analysis of Buildings.* Anil K. Chopra, Rakesh K. Goel, and Chatpan Chintanapakdee. December 2001.

PEER 2001/15 *Damage to Bridges during the 2001 Nisqually Earthquake.* R. Tyler Ranf, Marc O. Eberhard, and Michael P. Berry. November 2001.

PEER 2001/14 *Rocking Response of Equipment Anchored to a Base Foundation.* Nicos Makris and Cameron J. Black. September 2001.

PEER 2001/13 *Modeling Soil Liquefaction Hazards for Performance-Based Earthquake Engineering*. Steven L. Kramer and Ahmed-W. Elgamal. February 2001.

PEER 2001/12 *Development of Geotechnical Capabilities in OpenSees*. Boris Jeremić. September 2001.

PEER 2001/11 *Analytical and Experimental Study of Fiber-Reinforced Elastomeric Isolators*. James M. Kelly and Shakhzod M. Takhirov. September 2001.

PEER 2001/10 *Amplification Factors for Spectral Acceleration in Active Regions.* Jonathan P. Stewart, Andrew H. Liu, Yoojoong Choi, and Mehmet B. Baturay. December 2001.

PEER 2001/09 *Ground Motion Evaluation Procedures for Performance-Based Design.* Jonathan P. Stewart, Shyh-Jeng Chiou, Jonathan D. Bray, Robert W. Graves, Paul G. Somerville, and Norman A. Abrahamson. September 2001.

PEER 2001/08 *Experimental and Computational Evaluation of Reinforced Concrete Bridge Beam-Column Connections for Seismic Performance*. Clay J. Naito, Jack P. Moehle, and Khalid M. Mosalam. November 2001.

PEER 2001/07 *The Rocking Spectrum and the Shortcomings of Design Guidelines.* Nicos Makris and Dimitrios Konstantinidis. August 2001.

PEER 2001/06 *Development of an Electrical Substation Equipment Performance Database for Evaluation of Equipment Fragilities*. Thalia Agnanos. April 1999.

PEER 2001/05 *Stiffness Analysis of Fiber-Reinforced Elastomeric Isolators.* Hsiang-Chuan Tsai and James M. Kelly. May 2001.

PEER 2001/04 *Organizational and Societal Considerations for Performance-Based Earthquake Engineering*. Peter J. May. April 2001.

PEER 2001/03 *A Modal Pushover Analysis Procedure to Estimate Seismic Demands for Buildings: Theory and Preliminary Evaluation*. Anil K. Chopra and Rakesh K. Goel. January 2001.

PEER 2001/02 *Seismic Response Analysis of Highway Overcrossings Including Soil-Structure Interaction*. Jian Zhang and Nicos Makris. March 2001.

PEER 2001/01 *Experimental Study of Large Seismic Steel Beam-to-Column Connections.* Egor P. Popov and Shakhzod M. Takhirov. November 2000.

PEER 2000/10 *The Second U.S.-Japan Workshop on Performance-Based Earthquake Engineering Methodology for Reinforced Concrete Building Structures*. March 2000.

PEER 2000/09 *Structural Engineering Reconnaissance of the August 17, 1999 Earthquake: Kocaeli (Izmit), Turkey.* Halil Sezen, Kenneth J. Elwood, Andrew S. Whittaker, Khalid Mosalam, John J. Wallace, and John F. Stanton. December 2000.

PEER 2000/08 *Behavior of Reinforced Concrete Bridge Columns Having Varying Aspect Ratios and Varying Lengths of Confinement*. Anthony J. Calderone, Dawn E. Lehman, and Jack P. Moehle. January 2001.

PEER 2000/07 *Cover-Plate and Flange-Plate Reinforced Steel Moment-Resisting Connections.* Taejin Kim, Andrew S. Whittaker, Amir S. Gilani, Vitelmo V. Bertero, and Shakhzod M. Takhirov. September 2000.

PEER 2000/06 *Seismic Evaluation and Analysis of 230-kV Disconnect Switches.* Amir S. J. Gilani, Andrew S. Whittaker, Gregory L. Fenves, Chun-Hao Chen, Henry Ho, and Eric Fujisaki. July 2000.

PEER 2000/05 *Performance-Based Evaluation of Exterior Reinforced Concrete Building Joints for Seismic Excitation*. Chandra Clyde, Chris P. Pantelides, and Lawrence D. Reaveley. July 2000.

PEER 2000/04 *An Evaluation of Seismic Energy Demand: An Attenuation Approach*. Chung-Che Chou and Chia-Ming Uang. July 1999.

PEER 2000/03 *Framing Earthquake Retrofitting Decisions: The Case of Hillside Homes in Los Angeles.* Detlof von Winterfeldt, Nels Roselund, and Alicia Kitsuse. March 2000.

PEER 2000/02 *U.S.-Japan Workshop on the Effects of Near-Field Earthquake Shaking*. Andrew Whittaker, Editor. July 2000.

PEER 2000/01 *Further Studies on Seismic Interaction in Interconnected Electrical Substation Equipment.* Armen Der Kiureghian, Kee-Jeung Hong, and Jerome L. Sackman. November 1999.

PEER 1999/14 *Seismic Evaluation and Retrofit of 230-kV Porcelain Transformer Bushings*. Amir S. Gilani, Andrew S. Whittaker, Gregory L. Fenves, and Eric Fujisaki. December 1999.

PEER 1999/13 *Building Vulnerability Studies: Modeling and Evaluation of Tilt-up and Steel Reinforced Concrete Buildings*. John W. Wallace, Jonathan P. Stewart, and Andrew S. Whittaker, Editors. December 1999.

PEER 1999/12 *Rehabilitation of Nonductile RC Frame Building Using Encasement Plates and Energy-Dissipating Devices*. Mehrdad Sasani, Vitelmo V. Bertero, James C. Anderson. December 1999.

PEER 1999/11 *Performance Evaluation Database for Concrete Bridge Components and Systems under Simulated Seismic Loads*. Yael D. Hose and Frieder Seible. November 1999.

PEER 1999/10 *U.S.-Japan Workshop on Performance-Based Earthquake Engineering Methodology for Reinforced Concrete Building Structures*. December 1999.

PEER 1999/09 *Performance Improvement of Long Period Building Structures Subjected to Severe Pulse-Type Ground Motions*. James C. Anderson, Vitelmo V. Bertero, and Raul Bertero. October 1999.

PEER 1999/08 *Envelopes for Seismic Response Vectors.* Charles Menun and Armen Der Kiureghian. July 1999.

PEER 1999/07 *Documentation of Strengths and Weaknesses of Current Computer Analysis Methods for Seismic Performance of Reinforced Concrete Members*. William F. Cofer. November 1999.

PEER 1999/06 *Rocking Response and Overturning of Anchored Equipment under Seismic Excitations*. Nicos Makris and Jian Zhang. November 1999.

PEER 1999/05 *Seismic Evaluation of 550 kV Porcelain Transformer Bushings.* Amir S. Gilani, Andrew S. Whittaker, Gregory L. Fenves, and Eric Fujisaki. October 1999.

PEER 1999/04 *Adoption and Enforcement of Earthquake Risk-Reduction Measures.* Peter J. May, Raymond J. Burby, T. Jens Feeley, and Robert Wood. August 1999.

PEER 1999/03 *Task 3 Characterization of Site Response General Site Categories*. Adrian Rodriguez-Marek, Jonathan D. Bray and Norman Abrahamson. February 1999.

PEER 1999/02 *Capacity-Demand-Diagram Methods for Estimating Seismic Deformation of Inelastic Structures: SDF Systems*. Anil K. Chopra and Rakesh Goel. April 1999.

PEER 1999/01 *Interaction in Interconnected Electrical Substation Equipment Subjected to Earthquake Ground Motions*. Armen Der Kiureghian, Jerome L. Sackman, and Kee-Jeung Hong. February 1999.

PEER 1998/08 *Behavior and Failure Analysis of a Multiple-Frame Highway Bridge in the 1994 Northridge Earthquake*. Gregory L. Fenves and Michael Ellery. December 1998.

PEER 1998/07 *Empirical Evaluation of Inertial Soil-Structure Interaction Effects.* Jonathan P. Stewart, Raymond B. Seed, and Gregory L. Fenves. November 1998.

PEER 1998/06 *Effect of Damping Mechanisms on the Response of Seismic Isolated Structures*. Nicos Makris and Shih-Po Chang. November 1998.

PEER 1998/05 *Rocking Response and Overturning of Equipment under Horizontal Pulse-Type Motions*. Nicos Makris and Yiannis Roussos. October 1998.

PEER 1998/04 *Pacific Earthquake Engineering Research Invitational Workshop Proceedings, May 14–15, 1998: Defining the Links between Planning, Policy Analysis, Economics and Earthquake Engineering*. Mary Comerio and Peter Gordon. September 1998.

PEER 1998/03 *Repair/Upgrade Procedures for Welded Beam to Column Connections*. James C. Anderson and Xiaojing Duan. May 1998.

PEER 1998/02 *Seismic Evaluation of 196 kV Porcelain Transformer Bushings.* Amir S. Gilani, Juan W. Chavez, Gregory L. Fenves, and Andrew S. Whittaker. May 1998.

PEER 1998/01 *Seismic Performance of Well-Confined Concrete Bridge Columns.* Dawn E. Lehman and Jack P. Moehle. December 2000.

ONLINE PEER REPORTS

The following PEER reports are available by Internet only at http://peer.berkeley.edu/publications/peer_reports_complete.html.

PEER 2012/103 *Performance-Based Seismic Demand Assessment of Concentrically Braced Steel Frame Buildings.* Chui-Hsin Chen and Stephen A. Mahin. December 2012.

PEER 2012/102 *Procedure to Restart an Interrupted Hybrid Simulation: Addendum to PEER Report 2010/103.* Vesna Terzic and Bozidar Stojadinovic. October 2012.

PEER 2012/101 *Mechanics of Fiber Reinforced Bearings.* James M. Kelly and Andrea Calabrese. February 2012.

PEER 2011/107 *Nonlinear Site Response and Seismic Compression at Vertical Array Strongly Shaken by 2007 Niigata-ken Chuetsu-oki Earthquake.* Eric Yee, Jonathan P. Stewart, and Kohji Tokimatsu. December 2011.

PEER 2011/106 *Self Compacting Hybrid Fiber Reinforced Concrete Composites for Bridge Columns.* Pardeep Kumar, Gabriel Jen, William Trono, Marios Panagiotou, and Claudia Ostertag. September 2011.

PEER 2011/105 *Stochastic Dynamic Analysis of Bridges Subjected to Spacially Varying Ground Motions.* Katerina Konakli and Armen Der Kiureghian. August 2011.

PEER 2011/104 *Design and Instrumentation of the 2010 E-Defense Four-Story Reinforced Concrete and Post-Tensioned Concrete Buildings.* Takuya Nagae, Kenichi Tahara, Taizo Matsumori, Hitoshi Shiohara, Toshimi Kabeyasawa, Susumu Kono, Minehiro Nishiyama (Japanese Research Team) and John Wallace, Wassim Ghannoum, Jack Moehle, Richard Sause, Wesley Keller, Zeynep Tuna (U.S. Research Team). June 2011.

PEER 2011/103 *In-Situ Monitoring of the Force Output of Fluid Dampers: Experimental Investigation.* Dimitrios Konstantinidis, James M. Kelly, and Nicos Makris. April 2011.

PEER 2011/102 *Ground-Motion Prediction Equations 1964–2010.* John Douglas. April 2011.

PEER 2011/101 *Report of the Eighth Planning Meeting of NEES/E-Defense Collaborative Research on Earthquake Engineering.* Convened by the Hyogo Earthquake Engineering Research Center (NIED), NEES Consortium, Inc. February 2011.

PEER 2010/111 *Modeling and Acceptance Criteria for Seismic Design and Analysis of Tall Buildings.* Task 7 Report for the Tall Buildings Initiative - Published jointly by the Applied Technology Council. October 2010.

PEER 2010/110 *Seismic Performance Assessment and Probabilistic Repair Cost Analysis of Precast Concrete Cladding Systems for Multistory Buildlings.* Jeffrey P. Hunt and Božidar Stojadinovic. November 2010.

PEER 2010/109 *Report of the Seventh Joint Planning Meeting of NEES/E-Defense Collaboration on Earthquake Engineering. Held at the E-Defense, Miki, and Shin-Kobe, Japan, September 18–19, 2009.* August 2010.

PEER 2010/108 *Probabilistic Tsunami Hazard in California.* Hong Kie Thio, Paul Somerville, and Jascha Polet, preparers. October 2010.

PEER 2010/107 *Performance and Reliability of Exposed Column Base Plate Connections for Steel Moment-Resisting Frames.* Ady Aviram, Božidar Stojadinovic, and Armen Der Kiureghian. August 2010.

PEER 2010/106 *Verification of Probabilistic Seismic Hazard Analysis Computer Programs.* Patricia Thomas, Ivan Wong, and Norman Abrahamson. May 2010.

PEER 2010/105 *Structural Engineering Reconnaissance of the April 6, 2009, Abruzzo, Italy, Earthquake, and Lessons Learned.* M. Selim Günay and Khalid M. Mosalam. April 2010.

PEER 2010/104 *Simulating the Inelastic Seismic Behavior of Steel Braced Frames, Including the Effects of Low-Cycle Fatigue.* Yuli Huang and Stephen A. Mahin. April 2010.

PEER 2010/103 *Post-Earthquake Traffic Capacity of Modern Bridges in California*. Vesna Terzic and Božidar Stojadinović. March 2010.

PEER 2010/102 *Analysis of Cumulative Absolute Velocity (CAV) and JMA Instrumental Seismic Intensity (I_{JMA}) Using the PEER–NGA Strong Motion Database.* Kenneth W. Campbell and Yousef Bozorgnia. February 2010.

PEER 2010/101 *Rocking Response of Bridges on Shallow Foundations.* Jose A. Ugalde, Bruce L. Kutter, and Boris Jeremic. April 2010.

PEER 2009/109 *Simulation and Performance-Based Earthquake Engineering Assessment of Self-Centering Post-Tensioned Concrete Bridge Systems.* Won K. Lee and Sarah L. Billington. December 2009.

PEER 2009/108 *PEER Lifelines Geotechnical Virtual Data Center.* J. Carl Stepp, Daniel J. Ponti, Loren L. Turner, Jennifer N. Swift, Sean Devlin, Yang Zhu, Jean Benoit, and John Bobbitt. September 2009.

PEER 2009/107 *Experimental and Computational Evaluation of Current and Innovative In-Span Hinge Details in Reinforced Concrete Box-Girder Bridges: Part 2: Post-Test Analysis and Design Recommendations.* Matias A. Hube and Khalid M. Mosalam. December 2009.

PEER 2009/106 *Shear Strength Models of Exterior Beam-Column Joints without Transverse Reinforcement.* Sangjoon Park and Khalid M. Mosalam. November 2009.

PEER 2009/105 *Reduced Uncertainty of Ground Motion Prediction Equations through Bayesian Variance Analysis.* Robb Eric S. Moss. November 2009.

PEER 2009/104 *Advanced Implementation of Hybrid Simulation.* Andreas H. Schellenberg, Stephen A. Mahin, Gregory L. Fenves. November 2009.

PEER 2009/103 *Performance Evaluation of Innovative Steel Braced Frames.* T. Y. Yang, Jack P. Moehle, and Božidar Stojadinovic. August 2009.

PEER 2009/102 *Reinvestigation of Liquefaction and Nonliquefaction Case Histories from the 1976 Tangshan Earthquake.* Robb Eric Moss, Robert E. Kayen, Liyuan Tong, Songyu Liu, Guojun Cai, and Jiaer Wu. August 2009.

PEER 2009/101 *Report of the First Joint Planning Meeting for the Second Phase of NEES/E-Defense Collaborative Research on Earthquake Engineering.* Stephen A. Mahin et al. July 2009.

PEER 2008/104 *Experimental and Analytical Study of the Seismic Performance of Retaining Structures.* Linda Al Atik and Nicholas Sitar. January 2009.

PEER 2008/103 *Experimental and Computational Evaluation of Current and Innovative In-Span Hinge Details in Reinforced Concrete Box-Girder Bridges. Part 1: Experimental Findings and Pre-Test Analysis.* Matias A. Hube and Khalid M. Mosalam. January 2009.

PEER 2008/102 *Modeling of Unreinforced Masonry Infill Walls Considering In-Plane and Out-of-Plane Interaction.* Stephen Kadysiewski and Khalid M. Mosalam. January 2009.

PEER 2008/101 *Seismic Performance Objectives for Tall Buildings.* William T. Holmes, Charles Kircher, William Petak, and Nabih Youssef. August 2008.

PEER 2007/101 *Generalized Hybrid Simulation Framework for Structural Systems Subjected to Seismic Loading*. Tarek Elkhoraibi and Khalid M. Mosalam. July 2007.

PEER 2007/100 *Seismic Evaluation of Reinforced Concrete Buildings Including Effects of Masonry Infill Walls.* Alidad Hashemi and Khalid M. Mosalam. July 2007.

The Pacific Earthquake Engineering Research Center (PEER) is a multi-institutional research and education center with headquarters at the University of California, Berkeley. Investigators from over 20 universities, several consulting companies, and researchers at various state and federal government agencies contribute to research programs focused on performance-based earthquake engineering.

These research programs aim to identify and reduce the risks from major earthquakes to life safety and to the economy by including research in a wide variety of disciplines including structural and geotechnical engineering, geology/seismology, lifelines, transportation, architecture, economics, risk management, and public policy.

PEER is supported by federal, state, local, and regional agencies, together with industry partners.

PEER Core Institutions:
University of California, Berkeley (Lead Institution)
California Institute of Technology
Oregon State University
Stanford University
University of California, Davis
University of California, Irvine
University of California, Los Angeles
University of California, San Diego
University of Southern California
University of Washington

PEER reports can be ordered at http://peer.berkeley.edu/publications/peer_reports.html or by contacting

Pacific Earthquake Engineering Research Center
University of California, Berkeley
325 Davis Hall, Mail Code 1792
Berkeley, CA 94720-1792
Tel: 510-642-3437
Fax: 510-642-1655
Email: peer_editor@berkeley.edu

ISSN 1547-0587X